Accelerating shrinkage of Patagonian glaciers from the "Little Ice Age" (c. AD 1870) to 2011

B. J. Davies*, N. F. Glasser

*Corresponding author. Tel: 01970 622786. Email: bdd@aber.ac.uk

Both at: Institute for Geography and Earth Sciences, Aberystwyth University, Llandinam Building, Penglais Campus, Aberystwyth SY23 3DB, Wales, UK.

ABSTRACT. In this paper we used "Little Ice Age" ("LIA") trimlines and moraines to assess changes in South American glaciers over the last ~140 years. We determined the extent and length of 640 glaciers during the "LIA" (c. AD 1870) and 626 glaciers (the remainder having entirely disappeared) in 1986, 2001 and 2011. The calculated reduction in glacier area between the "LIA" and 2011 is -4131 km^2 (-15.4%), with -660 km^2 (-14.2%) being lost from the Northern Patagonian Icefield (NPI), -1643 km^2 (-11.4%) from the Southern Patagonian Icefield (SPI), and -306 km^2 (-14.4%) from Cordillera Darwin. Latitude, size and terminal environment (calving or land-terminating) exert the greatest control on rates of shrinkage. Small, northerly, land-terminating glaciers shrank fastest. Annual rates of area loss increased dramatically after 2001 for mountain glaciers north of 52°S and the large ice fields, with the NPI and SPI now shrinking at -9.4 km^2 a^{-1} (-0.23% a^{-1}) and -20.5 km^2 a^{-1} (-0.15% a^{-1}) respectively. The shrinkage of glaciers between 52°S and 54°S accelerated after 1986, and rates of shrinkage from 1986-2011 remained steady. Icefield outlet glaciers, isolated glaciers and ice caps south of 54°S shrank faster from 1986-2001 than they did from 2001-2011.

1. INTRODUCTION

1.1 Rationale

The glaciers of the Patagonian Andes and Tierra del Fuego region are currently shrinking rapidly. Regional assessments of glacier shrinkage is, however, only short-term because they are limited by the temporal availability of satellite observations (~40 years), aerial photography (~60 years) and detailed cartography (~60 years) required to produce accurate reconstructions of former glacier extent. Furthermore, inventories and assessments of modern glacier change in Patagonia have generally been restricted to individual glaciers (e.g. Harrison and Winchester, 2000; Stueffer and others, 2007), or geographically limited to one or two of the large icefields (e.g., Rivera and Cassassa, 2004; Bown and Rivera, 2007; Chen and others, 2007; Schneider and others, 2007; Lopez and others, 2010; Willis and others, 2011). Large parts of the southern Andes still

lack detailed inventories (cf. Masiokas and others, 2009b). There are no detailed assessments that encompass the entire region, covering both historically documented shrinkage and remotely sensed observations of change in recent decades. This paper therefore aims, firstly, to establish rates of glacier shrinkage from the "Little Ice Age" ("LIA") to the present day across southern South America, and secondly, to determine how rates of shrinkage changed through the late twentieth and early twenty-first centuries.

We here present a long (140 years) and spatially wide (2000 km in length) record of glacier change in South America (41° to 56°S) by calculating changes in glacier length and area between the end of the "Little Ice Age" (c. AD 1870), and the years 1986, 2001 and 2011. This is the first study to compare length and area changes since the "LIA" with change in recent decades for the whole study region. We also analyse spatial and temporal variability in glacier change and the controls thereupon. Our data is available from the Global Land-Ice Measurements from Space (GLIMS) database (www.glims.org).

1.2 Study area

The Andes are the longest continental mountain range in the world, stretching 7000 km along the coast of South America and reaching almost 7000 m a.s.l. in altitude. In our study area, the mountains reach a maximum of 4000 m a.s.l., decreasing to 1500-2000 m in southernmost South America. Between 38^{o} S and 56^{o} S there are four major ice masses (the Northern and Southern Patagonian Icefields, Gran Campo Nevado [GCN] and the Cordillera Darwin) and numerous snow- and ice-capped volcanoes and icefields (Fig. 1). Our study area focuses on the Patagonian Andes and Tierra del Fuego, from 41°S to 56°S. This region has had numerous detailed local studies covering glacier behaviour over various timescales, and there is good historical and geomorphological evidence for glacier fluctuations since the LIA (summarised by Masiokas and others, 2009b).

The Chilean Lake District (38-42°S) is characterised by shrinking glaciers on active volcanic cones, with frequent ash deposition insulating the ice. These volcano ice caps have been thinning since observations began in 1961, with more rapid thinning from 1981-1998. Their negative mass balances were caused by decreased precipitation and upper tropospheric warming over the last 30 years (Bown and Rivera, 2007). Equilibrium line altitudes are at approximately 1600 m at 43°S (Rivera and others, 2012). Glaciers north of 42°S receive higher precipitation during winter months than glaciers between 42°S and 49°S (Sagredo and Lowell, 2012).

The Northern Patagonian Icefield (NPI) covers an area of approximately 4200 km^2 at 47°S (Fig. 2a). Its survival at such a low latitude is attributed to a large volume of precipitation (up to 10,000 mm a^{-1} water equivalent) and to the cool temperatures associated with the high elevation of the Andes (Rott and others,

1998; Michel and Rignot, 1999; see temperature transects on Fig. 1). The NPI is characterised by high ablation rates, steep mass balance and precipitation gradients, and high ice velocities (Lopez and others, 2010). The glaciers of the NPI extend below the 0°C isotherm, and the snowline is generally below 2000 m a.s.l. (Sagredo and Lowell, 2012). The recent fluctuations of NPI outlet glaciers have been extensively studied (Aniya, 1988, 1995, 1996, 1999, 2001, 2007; Harrison and Winchester, 2000; Araneda and others, 2007; Chen and others, 2007; Lopez and others, 2010). San Rafael Glacier is the only tidewater glacier of the NPI, and is significant because it is the world's lowest latitude tidewater glacier, and is among the fastest flowing glaciers in the world (Warren and others, 1995; Koppes and others, 2011). Peak velocities of 19.7 ± 1.2 m per day were observed in 2007 by Willis and others (2011). Laguna San Rafael is dammed by large arcuate moraines that were formed during a mid-Holocene readvance of the glacier (Fig. 2b; Harrison and others, 2012).

The Southern Patagonian Icefield (SPI) stretches along the southern Andes, reaching altitudes of 3400 m. It is drained by temperate outlet glaciers, terminating on land or in proglacial lakes or tidal fjords (Aniya and others, 1997). Variations in glacier frontal positions have been studied since the 1940s, with long-term retreat (Aniya and others, 1992, 1996, 1997; Aniya, 1996, 1999; Lopez and others, 2010) and thinning (Aniya, 1995; Naruse and others, 1997; Naruse and Skvarca, 2000) being evident in the majority of the glaciers. Glaciers are generally larger than in the NPI, and Glaciar Pio XI is the largest in South America (1265 km^2) (Aniya and others, 1996).

The NPI and SPI have been shrinking dramatically ever since their “LIA” maxima, which is securely dated to AD 1870 (Glasser and others, 2011), and are now shrinking at an increasing rate in response to regional climate change. Rignot and others (2003) estimated that the two icefields jointly contributed 0.042 ± 0.002 mm a^{-1} to global mean sea level rise in the period 1968/1975 to 2000 but that this doubled to 0.105 ± 0.011 mm a^{-1} from 1995-2000. Chen and others (2007) estimated the ice loss rate for the Patagonia Icefields from 2002-2006 to be -27.9 ± 11 km^3 a^{-1}, equivalent to an average loss of ∼-1.6 m a^{-1} ice thickness change if evenly distributed over the entire glacier area and a global contribution to sea level rise of 0.078 ± 0.031 mm a^{-1}. Ivins and others (2011) estimated ice loss rates for the NPI and SPI of -26 ± 6 Gt a^{-1} from 2003-2009, using a combination of data from the GRACE satellite and GPS bedrock uplift data. The background to these changes is presumed to be the global surface temperature increase of 0.6 ± 0.2°C in the last century (Vaughan and others, 2001) resulting in widespread glacier wastage and shrinkage (Aniya, 1988; Ramirez and others, 2001; Arendt and others, 2002; Meier and others, 2003; Cook and others, 2005, WGMS, 2008).

Gran Campo Nevado, at 53°S, is an ice cap with several steep outlet glaciers (199 km^2; Schneider and others, 2007; Fig. 1), which may mean that it responds faster to climatic changes than the NPI or SPI (Möller and others, 2007). This ice cap is at much lower altitudes than the NPI or SPI, with mountain summits from 1000

to 1700m high, and with outlet glaciers reaching sea level. Mean annual temperatures here are +5.7°C, but the ice cap survives because of extremely high precipitation (Möller and Schneider, 2008).

Isla Riesco (52°S) is about 130 km long and 50 km wide, with moderate precipitation on its eastern part (< 1000 mm a^{-1}), which is leeward of the Andes mountains. The western part of the island is within the main belt of the Andean mountains, with high precipitation rates (Fig. 1). The mountains reach 1830 m, with several small ice caps and mountain glaciers (Casassa and others, 2002). All these glaciers terminate on land, with the exception of a few small freshwater lakes.

Tierra del Fuego is an archipelago off southernmost South America (Fig. 1), with many small ice caps and mountain glaciers, as well as the Cordillera Darwin icefield. Cordillera Darwin is the most southerly icefield in the study region, at 54°30'S, with topography constraining the ice masses (in comparison to the NPI and SPI, where ice-sheds separate the catchments (Warren and Aniya, 1999)). The mountains reach 2469 m a.s.l., and many of the glaciers calve into the ocean. The area receives more precipitation than land to the east and north, and glaciers south of the ice divide receive far more precipitation than those north of the ice divide, as a result of the orographic rain shadow (Holmlund and Fuenzalida, 1995). The glaciers of Tierra del Fuego and Cordillera Darwin receive uniform precipitation throughout the year, and have an annual temperature range of ~7.4°C and a mean annual temperature of 1.2°C (Sagredo and Lowell, 2012). The mass balance of Martial Este Glacier in Tierra del Fuego was found to have been negative (-772 mm water equivalent per annum) from 1960 to 2006 (Buttstädt and others, 2009).

1.3 Regional climate

1.3.1 Precipitation

The climate of Patagonia is dominated by Southern Hemisphere westerlies and equatorial Pacific sea surface temperatures, which regulate the El Niño Southern Oscillation (ENSO) and the Pacific Decadal Oscillation (Aravena and Luckman, 2009; Garreaud and others, 2009). The Andean mountain chain is a significant orographic barrier to the predominant westerlies, which results in steep precipitation gradients across the mountain chain (Masiokas and others, 2008; cf. Fig. 1). Precipitation between 40°S and 43°S declined between 1950 and 2000 (Aravena and Luckman, 2009). Furthermore, ENSO events, which are associated with reduced precipitation, have become more frequent since 1976 (Giese and others 2002; Montecinos and Aceituno 2003; Bown and Rivera, 2007).

1.3.2 Temperature

Throughout the Andes, there has been a positive trend in the 0°C isotherm, with an ELA rise attributed to this warming. This warming is regionally variable, with slight cooling or non-significant warming in southern Chile after 1976 (Carrasco and others, 2008). Tree ring data from the Southern Andes dating back to AD 1640 show that twentieth century temperatures have been anomalously warm; the mean annual temperatures for 1900-1990 for the northern and southern sectors of the Andes are 0.53°C and 0.86°C warmer than the 1640-1899 means (Villalba, 1994).

In the Chilean Lake District (38°-42°S), the upper troposphere has been warming at 0.019 to 0.031°C a^{-1}. However, low altitude air temperature cooling has been detected at several meteorological stations, particularly Puerto Montt and stations further north (Bown and Rivera, 2007). After 1976, changes in the Pacific Decadal Oscillation were observed, with a period of increased temperatures across the southern Andes (Villalba and others, 2003). Sagredo and Lowell (2012) hypothesise that under a changing climatic regime, glaciers in the NPI, SPI and Cordillera Darwin would become increasingly sensitive southwards to mean temperature rises and more uniform precipitation throughout the year.

2. METHODS

2.1 Data

Orthorectified (Level 1G) Landsat TM images from 1985-1987 and Landsat ETM+ images from 2001-2002 and 2010-2011 were acquired pre-registered to UTM WGS 84, zone 18S projection (Appendix I). These images have a large swath (185 km) and reasonable spatial resolution (30 m), and a geopositional accuracy of better than ± 50 m (Tucker and others, 2004). The 2010-2011 images have striping artefacts, caused by failure of the Scan Line Corrector (SLC) on the Landsat sensor in 2003.

For the NPI, additional data were obtained for 1975 from Aniya (1988). These data originate from 1974/1975 vertical aerial photographs, which were used to create a map by the Instituto Geografico Militar, Chile, which was subsequently used in a glacier inventory by Aniya (1988).

Elevation data were derived from the Shuttle Radar Topographic Mission (SRTM) digital elevation model (DEM) version 4.1 (hereafter SRTM4), at 3 arcseconds resolution (90 m) (Jarvis and others, 2008), providing elevation data from February 2000 (Appendix II). Vertical and horizontal errors are approximately 10 m (Farr and others, 2007). SRTM4 is a void-filled DEM, which may introduce inaccuracies in areas of steep topography (Frey and Paul 2012; Reuter and others, 2007), but is suitable for use in glacier inventories (cf. Frey and Paul 2012). There is uncertainty in glacier elevation in our 2001 census as a result of differing times of image capture between the SRTM and Landsat data.

159

160 **2.2 Glacier digitisation for 1986, 2001 and 2011**

161 Our methods follow GLIMS protocols, with each glacier between 41° S and 56° S (Fig. 1; Table 1) being
162 manually digitised as a separate polygon (Rau and others, 2005; Raup and others, 2007a; 2007b; Paul and
163 others, 2009; Racoviteanu and others, 2009; Svoboda and Paul, 2009; Raup and Khalsa, 2010). We digitized
164 glacier outlines in a Geographical Information System (GIS) (ESRI ArcMap 9.3) at 1:10,000 scale using cloud-
165 and snow-free Landsat satellite images available from summer months in 1985-1986, 2000-2001 and 2010-
166 2011 (Appendix I). Using data from Aniya (1988), the extents of 38 outlet glaciers for the NPI were also
167 digitised for 1975. Ice divides on the icefields were determined from previous publications (Aniya, 1996,
168 1999; Aniya and others, 1996; Rignot and others, 2003; Bown and Rivera, 2007; Rivera and others, 2007;
169 Lopez and others, 2010), and downloaded from GLIMS where possible (e.g., Schneider and others, 2007) to
170 ensure consistency with other studies, or by using high points, nunataks, glaciological structures or breaks in
171 slope (cf. Glasser and Scambos, 2008; Davies and others, 2011; Table 1). All icefield outlet glaciers and ice
172 caps and all mountain glaciers that could be clearly discriminated in the satellite images (as distinct from
173 snow) and that were larger than 0.1 km^2 (because of image resolution and the danger of misclassification of
174 snow patches) were digitised in this study. Near the NPI, SPI, Cordillera Darwin and GCN, there are numerous
175 small isolated glaciers with a “Mountain glacier” classification, which have been considered separately
176 (Northern Patagonian mountain glaciers (NPMG); Southern Patagonian Mountain Glaciers (SPMG); Cordillera
177 Darwin Mountain Glaciers (CDMG); Gran Campo Nevado Mountain Glaciers (GCMG).

178

179 **2.3 Geomorphological mapping to determine "LIA" extent**

180 Glacier extent at the "LIA" was digitized for glaciers between 38° S and 56° S (Fig. 1) (see Glasser and others,
181 2011) for glaciers with clear trimlines and moraines. The "LIA" extent was inferred from geomorphological
182 evidence, including trimlines and terminal moraines in front of contemporary glaciers (e.g. Fig 2), which were
183 identified according to previously defined criteria (Table 1). The inferred "LIA" glacier extents were checked
184 against known "LIA" positions from published valley-scale dendrochronological and lichenometric dating
185 studies, for example, for the Chilean Lake District (Bown and Rivera, 2007), NPI (Villalba, 1994; Winchester
186 and Harrison, 2000; Harrison and Winchester, 2000; Glasser and others, 2002, 2004; Araneda and others,
187 2007; Harrison and others, 2007, 2012), SPI (Aniya, 1995, 1996; Masiokas and others, 2009a; 2009b; Rivera
188 and others, 2011), Gran Campo Nevado (Koch and Kilian, 2005) and Cordillera Darwin (Kuylenstierna and
189 others, 1996; Masiokas and others, 2009b). In situations where multiple trimlines or moraines exist, we drew
190 the "LIA" limit at the trimline or moraine closest to the contemporary glacier snout (see Fig. 2 for examples
191 from the NPI). At those glaciers where there is no visible evidence of shrinkage since the "LIA" or where the

"LIA" limits are ambiguous or difficult to establish, for example, for some fjord-terminating glaciers of the SPI, the limits are assumed to be the same as in 1975 or 1986 (the earliest possible data available). Our results are therefore minimum estimates of ice shrinkage over the time period ~AD 1870 to 2011.

2.4 Glacier attribute data

Attribute data for each glacier polygon includes a unique Local-ID (the same as that used in previous inventories, where appropriate), GLIMS ID (Raup and Khalsa, 2010), any established glacier name, X and Y coordinates of the centroid, surface area (km^2), primary classification (Rau and others, 2005), form, frontal characteristics, ID and acquisition date of the satellite image, analyst name and analysis time. For "LIA" polygons, any published evidence of "LIA" ice extent and associated references are also included. Glacier aspect (azimuth of the accumulation area; Evans, 2006) was estimated using vectors that follow the steepest part of the glacier accumulation area. Glacier length was measured for 520 glaciers according to standard procedures (Lopez and others, 2010; Davies and others, 2011), following the longest flow pathway from the highest point on the ice divide to the glacier tongue (see Fig. 2). Minimum, maximum and median elevations and slopes for the year 2000 were derived automatically for each glacier in the GIS following analysis of SRTM4 (cf. Paul and others, 2009; Frey and Paul 2012).

2.5 Uncertainty

Digitised glacier lengths and outlines are accurate to ± 30 m (i.e. ± one pixel). Accuracy may be less in the centre of icefields, where ground control points are scarce, but as the same ice divides are used for each year inventoried, the uncertainty that this introduces into relative change measurement is limited. There may be inaccuracies where snow cover on nunataks in the centre of the icefields or adjacent to the ice edges has been misclassified as ice. We used qualitative methods to identify errors in glaciers with seasonal snow or large deviations in area between each year mapped, and manually improved these with additional Landsat images. Indeed, seasonal snow cover is not a significant problem in Patagonia because of the strong seasonality, and there is very little lying snow in the summer months near the glacier snouts. Where snow and ice is difficult to discriminate, for example on snow-capped mountains and volcanoes, glaciers have not been digitised.

Other potential sources of uncertainty include ice divide and drainage basin identification, error in co-registration (Granshaw and Fountain, 2006), clouds and shadows, and delineation of debris-coved glaciers (Bolch and others, 2010). However, this uncertainty was limited with manual digitisation at resolutions up to 1:10,000 (see Table 1), which is more accurate than automatic classification (cf. Jiskoot and others, 2009), particularly when dealing with debris-covered glaciers (Paul, 2002). Automatic classification is particularly

useful and suitable when analysing larger datasets comprising 1000+ glaciers with clean ice. However, we acknowledge that delineating the boundary of debris-covered ice is very difficult with images of this resolution. A further source of error is the striping on Landsat ETM+ images taken after 2003, and it was necessary to interpolate across the stripes. This was mitigated by using numerous overlapping images, so that interpolating across large stripes near the margins of the image was not required.

Statistical quantification of errors is difficult without ground control points, high-resolution satellite images or ground-truthing in the week that the satellite image was taken (cf. Svoboda and Paul, 2009). In order to quantify uncertainty, we conducted error analysis of the digitisation of six NPI outlet glaciers in 1986 (i.e. the same glacier was independently digitised 5 times), both with and without debris cover and with grounded and floating termini (cf. Stokes and others, 2007). This yielded an average standard deviation of 0.3 km^2, or 2.0% of the area. Analysis of the area changes of glaciers is therefore considered to be accurate to within 2.0%. The glaciological uncertainty of ice divides is likely to be far larger than the mapping uncertainty, which has little influence on the final glacial outline, especially when comparing ice margin change from different years.

2.6 Analysis of glacier change

There are four kinds of data resulting from this study: **glacier descriptors** (area, length, primary classification, aspect, frontal characteristics, etc.); **length changes** (km and m per annum [m a^{-1}]); **area changes** (km^2 and per cent); and **annual rates of change**, which are expressed as a percentage (% a^{-1}; cf. Bolch and others, 2010). We use 'recession' where length changes are discussed and 'shrinkage' where area changes are discussed. Annual rates of change were calculated by dividing the area change by the time between analyses for each glacier (time is taken from the date the satellite image was acquired). The latter are the only result that can be directly compared between different time periods and different glaciers, because of the different lengths of time between analyses (i.e., ~116 years from 1870-1986; ~15 years from 1986-2001; ~10 years from 2001-2011, depending on when the satellite image for each glacier was acquired).

3. RESULTS

3.1 Characteristics of South American glaciers in 2011

In 2011, 626 glaciers were considered in our assessment, which included 386 major outlet glaciers from the main icefields (44 from the NPI, 161 from the SPI, 35 from GCN and 99 from Cordillera Darwin) (Table 2). These four principal icefields dominate the glacierised area (Fig. 3a). Glacier sizes in 2011 ranged from 0.1 km^2 to 1344 km^2 (SPI-137; Pio XI) (Table 2). Although there are many small glaciers, a few large glaciers comprised the majority of the glacierised area (Fig. 3a). The mountain ranges beneath the SPI, NPI, Gran

Camp Nevado and El Volcan are orientated north-south, resulting in a predominantly west-east aspect for the outlet glaciers (Fig. 3b).

In the study region there were 233 outlet, 95 valley and 229 mountain glaciers, 26 ice caps and 38 icefields, with outlet glaciers dominating the glacierised area. Although mountain glaciers are numerous, they comprised only a small proportion of the glacierised area (8.3%; Fig. 3c). Many of the valley or outlet glaciers have a compound basin (numerous cirques or catchment areas) or compound basins, where two compound basin drainage systems merge (Fig. 3d; Rau and others, 2005). The majority of the glaciers surveyed terminate on land (526), although 100 have calving termini (35 marine and 65 lacustrine).

Mean glacier elevation ranged from 496 m a.s.l. (IH-14) to 2182 m a.s.l. (MSL-5) (Table 2). Parque Nacional Vicente Perez Rosales (VPR-1) had the highest mean elevation (2158 m a.s.l.), and NPI-1 had the highest maximum elevation (3968 m a.s.l.). Overall, 41% of the glaciers had a median altitude of 1000-1500 m a.s.l., with only one glacier having a median altitude of 0-500 m or over 2000 m (Fig. 3e). There was a weak relationship ($r^2 = 0.2$) between maximum altitude and glacier area in 2001 (Fig. 3f), and there was a trend towards decreasing glacier median altitudes southwards (Fig. 3g; Table 2). There was a large scatter in glacier altitude, with large outlet glaciers from the ice fields having a wide range of median altitudes. Glacier slope varied with glacier length ($r^2 = 0.3$; Fig. 3h), which is important, as shorter, steeper glacier typically have the fastest response times (Raper and Braithwaite, 2009). Regionally, the steepest glaciers were found in Parque Nacional Vicente Perez Rosales, and the lowest mean slopes are found in the NPI and SPI (Table 2).

The NPI (4365 km^2) was 120 km long, 70 km at its widest, and extended from 46°30'S to 47°30'S. It had a mean altitude of 1340 m a.s.l.. We analysed 44 outlet glaciers of the NPI covering 3976 km^2 and 59 isolated nearby glaciers (NPMG, Cordon La Parvas, Cordillera Lago General Carrera) surrounding the NPI, covering 389 km^2. These mountainous regions generally had glaciers with high mean slopes and altitudes (Table 2). Nineteen of the outlet glaciers had calving termini, of which only one (Glaciar San Rafael) was marine-terminating. Glaciers west of the ice divide made up the majority of the glacierised area of the NPI (Table 3; Fig. 4a). The more southerly glaciers of El Volcan (cf. Fig. 1; Table 2) were primarily small ice caps and mountain glaciers with a mean altitude of 1521 m a.s.l., and all were land-terminating, though some have small lakes in their forefields.

The SPI was the largest icefield (13,219 km^2) and stretched north-south for 400 km, from 48°S to 52°S along the southern Andes, with widths between 30 and 70 km, and a mean altitude of 1191 m a.s.l.. In our assessment, it was drained by 154 outlet and simple basin glaciers with 45 nearby isolated glaciers (in SPMG, El Condor, Cerro Paine Grande, Torres Del Paine) covering 278 km^2. Its area was again dominated by glaciers west of the ice divide (Table 3), but with several large outlet glaciers draining eastwards. Of the outlet glaciers, 54 had calving termini, and they accounted for 10,945 km^2, or 83% of the total area (Fig. 4a).

Gran Campo Nevado (52°40'S to 52°55'S) was the smallest ice cap (262 km^2) with 35 glaciers (of which four calve into lakes), and was 24 km long and 16 km wide. It was surrounded by 17 small mountain glaciers and ice caps. Cordillera Darwin (1931 km^2) was the southernmost icefield (54°30'S), and was 90 km long and 30 km wide. There were 99 glaciers, of which 66 are outlet glaciers (covering 408 km^2). Ten of these had calving termini. There were 18 small isolated glaciers nearby, including 7 valley glaciers and 6 small icefields and ice caps nearby.

3.2 Changes in glacier length and area from 1870 to 2011

3.2.1 General trends

A total of 640 glaciers were digitised from 1870 from 40°S to 56°S (Figs. 4-6; Table 4). Of these, 626 remained in 1986. Overall, 90.2% of the glaciers shrank from 1870 to 2011, 0.3% advanced, and 9.5% showed no change. Despite some small advances, which are generally short-term and limited to tidewater glaciers, all regions have suffered extensive glacier surface area loss. For the SPI and the eastern NPI, the greatest rates of shrinkage were observed in land-terminating glaciers (Fig. 4a). Glacier shrinkage from 2001-2011 was greatest in those glaciers less than 5 km^2 in size, with those greater than 100 km^2 in particular having slow rates of shrinkage (Fig. 4b). Rate of shrinkage were also fastest in those glaciers furthest north, with most glaciers shrinking. Latitudinal gradients are also emphasised, with glaciers from 41-44°S generally all shrinking, small glaciers from 44-53°S also shrinking, and with little shrinkage in glaciers from 54-56°S (Fig. 4b). Mean glacier altitude and slope (Figs. 4c and 4d) had little control on glacier shrinkage in Patagonia.

Annualised rates of shrinkage across South America increased for each time period measured (Table 4; Fig. 4e), with overall rates of areal loss twice as rapid from 2001-2011 as from 1870-1986 (-0.10% a^{-1} for 1870-1986, -0.14% a^{-1} for 1986-2001, and -0.22% a^{-1} for 2001-2011). Across the study area, percentage change per annum was greatest from 1870-1986 for 212 glaciers, from 1986-2001 for 172 glaciers, and from 2001-2011 for 155 glaciers. Across the study region, 14 glaciers extant during the "LIA" had disappeared entirely by 1986, mostly around the SPI.

3.2.2 Mountain glaciers

In general, rates of change were fastest from 2001-2011 in the more northerly locations (Parque Nacional Vicente Perez Rosales, Hornopiren, Parque Nacional Corcovado, Cerro Hudson, and SPMG; Figs. 4e, 5), and faster from 1986-2001 in the more southerly locations (e.g., Cordillera Darwin, Isla Hosta, Monte Sarmiento, Isla Riesco, and Tierra del Fuego (cf. Fig. 1 for locations). North of 46°S, small, land-terminating glaciers are generally rapidly shrinking, and the rate of area loss is accelerating (Figs. 1, 4b, 4e, 5). Indeed, the ice caps of

the Chilean Lake District experienced some of the fastest rates of area loss in the area from 2001-2011 (Fig. 5; Table 4). Although there is little clear statistical relationship between glacierised area and rate of shrinkage, glaciers north of 52°S show increased relative rates of shrinkage. Out of 16 glaciers in the Parque Nacionale Corcovado, 11 shrank fastest from 2001-2011, 3 from 1986-2001, and 2 from 1870-1986. These more northerly glaciers also tend to be higher, steeper and smaller (Fig. 3g, 4b), which may result in shorter response times.

Between 52° and 46°S, rates of area loss were also generally faster from 2001-2011, although it is more variable. For the seven mountain glaciers of Cerro Erasmo, steady and accelerating glacier length recession was observed (Fig. 6a). All glaciers receded, but distances varied between -0.5 km and -5.6 km. Around the NPI, mountain glaciers receded rapidly between 1870-1986. For example, CLGC-6 receded 7.1 km (60 m a^{-1}) during this period, but thereafter length did not change. Northern Patagonian mountain glaciers (NPMG) had a total area loss of -1.2% from 2001-2011, Cordon La Parvas mountain glaciers lost -3.2%, and Cordillera Lago General Carrera glaciers lost -1.2% (Table 4).

Length fluctuations of 32 glaciers were measured for El Volcan. Some glaciers receded rapidly from 1870-1986 but have since remained stable (e.g., EV-14 [0.6 km or -5 m a^{-1}], EV-19 [-2.5 km or -22 m a^{-1}], EV-30 [-1.4 km or -12 m a^{-1}] and EV-32 [-1.0 km or -9 m a^{-1}]), but most have steadily receded (Fig. 6c). The glaciers that receded fastest were EV-37 (-63m a^{-1} from 1986-2001), EV-22 (-118 m a^{-1} from 2001-2011), EV-24 (-66 m a^{-1} from 2001-2011) and EV-28 (-22 m a^{-1} from 1870-1986). Rates of area loss peaked from 1986-2001 and then declined (Table 4).

For SPI mountain glaciers, the largest areal changes from 2001-2011 were for SPMG-5 (-3.83%), SPMG-15 (-5.03%), SPMG-7 (-1.12%) and EC-1 (-4.41%). Glaciers around the SPI, particularly south and east of the main icefield, shrank very rapidly after 2001 (Fig. 4e). From 2001-2011, the El Condor region had a reduction in glacier area of -44%; SPMG of -26.8%, and Lago del Desierto of -6.5% (Table 4). For these regions, rates of area loss are several orders of magnitude faster after 2001 (-2.37% a^{-1} for SPMG) compared with 1870-1986. However, the mountains of El Condor are heavily snow-covered, which may induce an over-estimation of glacierised area in 2001. There are also no trimlines or moraines mapped in this region, so extent during the "LIA" extents are not possible to estimate.

Between 52°S and 54°S there is more variation, with Gran Campo Nevado mountain glaciers shrinking fastest after 2001, but with the Monte Burney ice cap and Isla Riesco glaciers shrinking fastest from 1986-2001 (Fig. 4e). From 2001-2011, only two mountain glaciers around GCN shrank, with the remaining glaciers remaining stationary (Fig. 5). In Isla Riesco from 2001-2011, one glacier advanced (RI-1; +0.26% a^{-1}) and only one had significant shrinkage (RI-4, at -1.33% a^{-1}).

355 Mountain glaciers south of 54°S (Tierra del Fuego, Monte Sarmiento, Cordillera Darwin mountain glaciers
356 and Isla Hoste) generally shrank fastest from 1986-2001, and show little change after 2001 (cf. Figs. 4e, 5).

357

358 *3.2.3 Northern Patagonian Icefield (NPI)*

359 Almost all glaciers (98.1%) in the NPI shrank from 1870-2011. Length fluctuations were measured for 38 NPI
360 glaciers, and showed a general trend of increasing recession (Fig. 6b). Several glaciers were stable from
361 1986-2001, but receded from 2001-2011 (e.g., NPI-21 [Pared Norte; -112 m a^{-1}], NPI-20 [Pared Sur; -189 m a^{-1}] and NPI-2 [-112 m a^{-1}]). Still others receded at steadily increasing rates (e.g., NPI-10 [Strindberg] and NPI-14). NPI-7 (San Rafael; lagoonal) receded by -9.6 km [-83 m a^{-1}] between 1870 and 1986, and by a further -1.2 km by 1990, whereupon the margin stabilised.

365 The fastest rates of shrinkage east of the NPI ice divide were for land-terminating glaciers. West of the ice
366 divide, the fastest rates of shrinkage were observed in calving glaciers, which also occupy a larger area (Fig.
367 4a). The large areal losses of the NPI from 1870-2011 were dominated by a small number of large glaciers.
368 These include NPI-7 (-11.5%; San Rafael), NPI-8 (San Quintin; -14.6%) and NPI-25 (Colonia; -12.9%) (cf. Fig. 2).
369 Glaciers east of the ice divide shrank by -2.2% from 2001-2011 (Table 3), compared with -2.4% for glaciers of
370 the west. Four glaciers had small, short-term advances (NPI-14 from 1975-1986; NPI-32 from 1986-2001;
371 NPI-18 and NPI-86 from 2001-2011).

372 Overall, rates of area loss from 2001-2011 (-0.23% a^{-1}) were over twice that of 1870-1986 (-0.09% a^{-1}) (Fig.
373 4e), with similar rates both west and east of the ice divide (Table 3). However, more glaciers shrank fastest
374 from 1975-1986 than from 2001-2011 (Table 4). The rapid areal shrinkage from 2001-2011 of NPI-1 (Grosse;
375 -1.69% a^{-1}), NPI-6 (Gualas; -0.97% a^{-1}), NPI-16 (HPN-4; -0.26% a^{-1}) and NPI-25 (Colonia; -0.15% a^{-1}) dominates
376 the trend observed in Figure 4e, but in general, the small glaciers fringing the icefield shrank fastest (Figs. 4,
377 5, 6a). The period of most rapid shrinkage of the other glaciers is variable, from 1870-1986 (e.g., NPI-7; San
378 Rafael; -0.09% a^{-1}), to 1975-1986 (e.g., NPI-8; San Quintin; -0.23% a^{-1}), 1986-2001 (e.g., NPI-14 [-0.23% a^{-1}],
379 NPI-12 [Benito; -0.33% a^{-1}], and NPI-5 [Reicher; -0.77% a^{-1}]) (Figs. 2b; 2c; 7a). It is also clear from the scatter
380 plot in Fig. 5 that calving glaciers are currently shrinking less rapidly (as a percentage of their area per
381 annum) than land-terminating glaciers. Indeed, Fig. 4a shows that land-terminating glaciers have relative
382 rates of area loss much higher than calving glaciers, both east and west of the ice divide, with land-
383 terminating glaciers east of the ice divide shrinking at -0.27% a^{-1} from 2001-2011, compared with -0.11% a^{-1}
384 for calving glaciers. However, it should be noted that these large calving glaciers have lost the most area in
385 absolute terms, and are still shrinking rapidly.

386

3.2.4 Southern Patagonian Icefield (SPI)

For the SPI, 96.5% of the glaciers shrank from 1870-2011, with the majority (59 out of 154) shrinking fastest from 2001-2011. The length fluctuations of 157 glaciers show large but variable linear recession from their "LIA" maxima (e.g., SPI-14 [O'Higgins; -16.0 km by 2011; lacustrine] and SPI-1 [Jorge Montt; -10.0 km by 2001 followed by a small advance of 0.5 km 2001-2011]). Several large glaciers shrank particularly fast from 2001-2011 (e.g., SPI-142 [Occidental; -216 m a^{-1}], SPI-179 [-76 m a^{-1}], SPI-22 [-157 m a^{-1}]) (Fig. 6d).

The largest relative area changes (1870-2011) were generally from the smaller outlet glaciers, such as SPI-26 (-82.4%), SPI-177 (-85.8%) and SPI-169 (-93.2%). The larger outlet glaciers have also lost surface area from 1870-2011, for example, from SPI-1 (Jorge Montt ; -12.6%), SPI-14 (O'Higgins; -10.9%), SPI-31 (Upsala; -19.7%) and SPI-142 (Occidental; -11.5%). Three glaciers advanced from 1986-2001 (SPI-137 (+2.1 km^2); SPI-198 (+2.4 km^2) and SPI-77 (+0.3 km^2)) and three from 2001-2011 (SPI-113 (+4.9 km^2); SPI-109 (+0.6 km^2) and SPI-45 (+4.9 km^2)); in the case of SPI-113, the advance from 2001-2011 was beyond 1870 limits. However, it is difficult to determine the 1870 limit for fjord-type glaciers without moraines, such as SPI-113.

Overall, for the SPI, rates of area change were more than twice as rapid from 2001-2011 (-0.15% a^{-1}) than from 1870-1986 (-0.07% a^{-1}; Fig. 4e), but this result is again dominated by a small number of outlet glaciers (Fig. 5, 6b), particularly small ones south of the main icefield, such as SPI-70 (-1.22% a^{-1}); SPI-149 (-6.37% a^{-1}) and SPI-199 (-1.95% a^{-1}) (Fig. 6, 7b). Although some calving outlet glaciers are shrinking rapidly, for example, SPI-141 (-0.22% a^{-1}); SPI-145 (-1.02% a^{-1}) and SPI-31 (Upsala; -19.7% a^{-1}), in general, small, land-terminating glaciers are experiencing the fastest annual rates of shrinkage (Figs. 5, 6). Across the SPI, glaciers on the east of the ice divide had slightly faster annual rates of shrinkage (Table 3), with land-terminating glaciers shrinking at rates of -0.29% a^{-1} from 2001-2011, compared with -0.08% a^{-1} for calving glaciers west of the ice divide (Fig. 4a). Figure 7b illustrates the highly variable but rapid area loss in small glaciers around the fringes of the SPI, with particular large glaciers also losing surface area. Rates of area loss are increasing around the SPI, with most glaciers experiencing their fastest rates of area loss from 2001-2011 (Fig. 8b; Table 4). For most of the remaining glaciers, the period of fastest area loss was 1986-2001.

3.2.5 Gran Campo Nevado (GCN)

Around the GCN, 19 glaciers (36.5%) did not exhibit any change, 33 (63.5%) shrank and none advanced from 1870-2011. The 31 glaciers of GCN for which length was measured show, in general, recession, with various glaciers receding at different rates during each time period (Fig. 6e). While the mountain glaciers around GCN shrank rapidly after 2001, rates of area loss for land-terminating outlet glaciers have remained steady (Fig. 4e). Although most glaciers shrank from their "LIA" maxima, the fastest annual rates of shrinkage were observed in small glaciers (Fig. 5; 6c). In total, 11 glaciers shrank fastest from 1986-2001, and 10 from 2001-

2011 (Table 4). Annual rates of shrinkage were similar from 1986 to 2011 (-0.23% a^{-1}; Table 4; Fig. 4e; 8c). The glaciers losing area fastest from 2001-2011 were GCN-03 (-2.22% a^{-1}), GCN-27 (-1.17% a^{-1}) and GCN-51 (-5.53% a^{-1}). The large outlet glaciers had smaller rates of relative area loss; for example; GCN-26 [-0.53% a^{-1}] and GCN-42 [-0.37% a^{-1}] (Fig. 7c).

3.2.6 Cordillera Darwin

The numbers of glaciers shrinking in Cordillera Darwin fell from 77.5% from 1870-1986, 39.5% from 1986-2001, to 31.8% from 2001-2011, with many glaciers showing no change from 2001-2011. Glacier length was measured for 107 glaciers in the Cordillera Darwin, with most receding until 1986, and with little frontal change after this. Some calving glaciers had small advances between 1986 and 2011, for example, CD-80 (+1.3 km from 2001-2011; further than its 1986 limit). A lack of moraines makes the 1870 limit difficult to map. In contrast, CD-8, also marine terminating, receded rapidly from 1986-2001 (-756 m a^{-1}), after which recession slowed (-202 m a^{-1} from 2001-2011) (Fig. 6f).

Many glaciers had little or no shrinkage from 1870-2011, and the glaciers with the fastest annual rates were small and land-terminating (Figs. 5, 7c). Outlet glaciers of Cordillera Darwin had their fastest rates of area loss from 1986-2001 (Fig. 4e, 8d). Overall, rates of area loss were more than twice as fast from 1986-2001 (-0.26% a^{-1}) than from 1870-1986 (-0.08% a^{-1}), but they fell to -0.12% a^{-1} after 2001 (Table 4; Fig. 4e). 29 glaciers shrank fastest from 1986-2001, compared with 16 from 2001-2011 (Table 4).

The outlet glaciers of the nearby Monte Sarmiento and Isla Hoste ice caps show similar patterns, frequently with low rates of shrinkage (Figs. 5, 7d). Overall, for both ice caps, the period of fastest area loss was from 1986-2001, with many glaciers having no observable change after 2001 (Figs. 5, 8d; Table 4). It is again the small, land-terminating glaciers that are shrinking fastest (cf. Fig. 5).

4. DISCUSSION

4.1 Comparison with previous inventories

Our calculated area for NPI of 3976 km^2 in 2011 and 4070 km^2 in 2001 is similar to the previous estimate of a total ice area of 3953 km^2 in 2001 made by Rivera and others (2007). Our calculated area for the contemporary SPI of 13,219 km^2 in 2011 also fits with the previous estimate for this icefield of 13,000 km^2 (Aniya, 1999). For GCN, our calculated area of 243 km^2 in 2001 fits well with the calculated area of Schneider and others (2007) of 252.6 km^2 in 2002. Differences may be because we included more of the surrounding glaciers in our study.

Our data lend independent support to the assertion of Rignot and others (2003) and Glasser and others (2011) that the Patagonian icefields are shrinking at an increasing rate. Our calculated rates of area loss from the NPI suggest that there was an increase in annual area loss rates from -0.09% a^{-1} in the 116 years between AD 1870 and 1986, to -0.12% a^{-1} in the 15 years between 1986 and 2001, and -0.23% a^{-1} from 2001-2011 (Table 4).

4.2 Calving dynamics and asynchronous glacier change

The acceleration in relative rates of area loss from 2001-2011 for the NPI was dominated by the smaller land-terminating glaciers (cf. Figs. 4e, 5). The shrinkage of marine- and lacustrine-terminating glaciers is highly variable, and reflects a dynamic and non-linear response to multiple factors. For example, NPI-1, NPI-6, NPI-16 and NPI-25 terminate in freshwater lakes, and had particularly rapid rates of area loss. NPI-1, however, ablates not by calving but by rapid thinning and surface melting, with large supraglacial ponds (Masamu Aniya, Pers. Comm, May 2012). The fragmented snout of NPI-16 is difficult to define, which may induce an error in assessing the shrinkage. Supraglacial debris cover insulates the glacier from solar radiation and so affects ablation rates (Scherler and others, 2011). For example, slow shrinkage of NPI-1 (Glaciar Grosse) prior to 2001 was attributed to insulation by thick debris cover (Aniya, 2001). The floating terminus of NPI-6 (Glaciar Gualas) advanced from 1996-1999, possibly as a result of stretching (Aniya, 2001). This stretching was followed by more rapid shrinkage from 2001-2011, driven by rapid calving induced by large, deep, water-filled crevasses.

NPI-7 (Glaciar San Rafael), NPI-8 (Glaciar San Quintin) and NPI-5 (Glaciar Reicher) (Figs. 2, 7, 8) shrank most rapidly from 1870-1986, 1986-2001 and 1986-2001 respectively. These lacustrine-terminating glaciers are the largest of the NPI and have widely different accumulation area ratios. They have shown repeated still stands, advances and retreats since the 1920s (Winchester and Harrison, 1996; Aniya 2007, Araneda and others, 2007; Lopez and others, 2010). Glaciar San Rafael currently has a high velocity and is thinning extensively (Willis and others, 2011). Steady thinning of the glacier surface could induce periodic floatation and rapid retreat, followed by grounding and stabilisation (Aniya, 2007). An advance reported from 1992 to 1999 for Glaciar San Rafael (Aniya, 2001) explains the reduced area loss rates observed from 1986-2001. Glaciar San Quintin terminated on land until 1991, when shrinkage led to the formation of a lake in the former glacier basin, into which it now calves (Rivera and others 2007; Willis and others, 2011). Large-scale shrinkage was observed in Glaciar Reicher from 1996-1999 (Aniya, 2001), before the glacier appeared to reach a new equilibrium. NPI-12 (Glaciar Benito) and NPI-13 (HPN-1) are both thinning rapidly and accelerated in speed between 2007-2011 (Willis and others, 2011). Neither glacier has shown significant shrinkage in this period.

For the SPI, the acceleration of shrinkage post-2001 is dominated by smaller fringing glaciers (Figs. 4e, 5, 7b, 8b). However, the majority of the large outlet glaciers draining the SPI calve into freshwater lakes or fjords, with highly variable behaviour in each catchment basin (Aniya, 1995; Fig. 8d). Dynamical changes in the calving glaciers of the SPI are discussed below.

SPI-31 (Glaciar Upsala) calves into a lake on the eastern SPI and shrank at -0.2% a^{-1} from 2001-2011. Previous studies observed thinning (-33 m between 1990 and 1993; Naruse and Skvarca, 2000) and rapid area loss, and argued that this was caused by variations in bed topography, with bedrock rises in the lake controlling frontal fluctuations (Naruse and others, 1997; Naruse and Skvarca, 2000). SPI-137 (Pio XI) is currently shrinking at a rate of -0.04% a^{-1}. From 1986-2001, Pio XI advanced at a rate of +0.01% a^{-1}, with a documented advance of up to +10 km from 1945-1986 (Rivera and Cassassa, 1999), with thickening by an average of +44.1 m from 1975-1995.

SPI-16 (Glaciar Chico) is shrinking slower than many of the other large tidewater glaciers of the SPI (at -0.18% a^{-1}), which has been attributed to limited calving activity (Rivera and others, 2005). However, this glacier is thinning at rates comparable to other glaciers of the SPI, and the rate of area loss has accelerated in each successive period. SPI-14 (Glaciar O'Higgins) shrank most rapidly from 1870-1986 (-0.09% a^{-1}), followed by slower shrinkage from 1986-2001 (-0.02% a^{-1}) and from 2001-2011 (-0.01% a^{-1}). This is largely due to a rapid retreat of -4.7 km from 1973-1976 (Lopez and others, 2010).

SPI-48 (Glaciar Perito Moreno), on the eastern side of the ice divide, calves into Lago Argentino (cf. Fig. 8b), with only limited area loss (-0.1%) after 2001. This glacier is well known for periodic advances and retreats, related to the geometry of its calving front. The glacier periodically advances to Península Magallanes, whereupon it dams the lake. Rising lake levels lead to increased pressure and eventual ice-dam and lake-drainage events through the ice front (Stueffer and others, 2007).

Therefore, across the NPI and SPI, atmospheric temperature changes have led to thinning, resulting in calving glaciers reaching floatation point and becoming unstable (cf. Rivera and Cassassa, 2004). Stretching may cause short-lived advances, but encourages thinning and enhanced calving, resulting eventually in retreat. Accelerated retreat may occur after shrinkage from a pinning point (Holmlund and Fuenzalida, 1995; Warren and Aniya, 1999). Alternatively, a marine shoal may reduce water depths and encourage advance. The formation of a proglacial lake may accelerate glacier shrinkage, but if the glacier retreats beyond the lake margin, shrinkage may slow down. Therefore glacier shrinkage in calving glaciers is regulated by individual dynamics (calving status, equilibrium line altitude, channel geometry (Aniya and others, 1997)), with retreating, advancing and stable termini observed.

4.3 Temporal and regional variations

From Figures 4 and 5, it is clear that latitude, size and terminal environment exert the greatest controls on glacier shrinkage, with the more northerly, smaller, land-terminating glaciers shrinking fastest. Calving glaciers are changing in area (relative rates of area loss) more slowly than small land-terminating glaciers, with internal calving dynamics controlling tidewater termini (cf. Fig. 4a). The spikes in SPMG and El Condor are caused by a small number of very rapidly shrinking glaciers, such as EC-1, SPMG-15 and SPMG-5. Worldwide, small glaciers and ice caps have reacted particularly dynamically to increased global temperatures (Oerlemans and Fortuin, 1992; Hock and others, 2009), and it has been proposed that the volume loss from mountain glaciers and ice caps like these is the main contributor to recent global sea level rise (Church and others, 2001; Braithwaite and Raper, 2002; Meier and others, 2007; Hock and others, 2009). On a regional scale, both the large icefields and small ice caps and glaciers north of 52°S have suffered accelerated shrinkage from 2001-2011 (Fig. 4e), presumably driven by the observed increases in upper tropospheric air temperatures since 1976, particularly at Puerto Montt (Giese and others, 2002; Villalba and others, 2003; Bown and Rivera 2007; Carrasco and others, 2008; Aravena and Luckman, 2009; Rivera and others, 2012). Glacierised summits in the Chilean Lake District lie within this altitudinal zone, and so this warming is likely to be a significant control on the mass balance of ice caps and glaciers between 41° and 46°S in the far north of the study region, resulting in rapid shrinkage (i.e., Parque Nacional Vicente Rosales, Hornopieren, and Parques Nacional Corcovado and Quelat).

There is a very slight east-west gradient in annual rates of area loss for the NPI and SPI (Table 3), in particular for the period 1870-1986, with the eastern glaciers shrinking fastest. This is illustrated further by Figure 6, where smaller glaciers on the east of the NPI and the nearby glaciers exhibit the fastest rates of relative shrinkage. We do not find strong evidence for shrinkage gradients in the outlet glaciers after 1986; this contrasts with other studies, where it has been argued that changes in precipitation are driving the accelerated shrinkage east of the ice divide (cf. Aravena and Luckman, 2009). However, it should be noted that absolute rates of area loss (km^2 per annum) are higher on the west of the ice divide, due to the larger glacierised area here. Harrison and Winchester (2000) also found little evidence of clear east-west gradients or patterns of behaviour for the NPI. It is possible that declining precipitation drove increased relative shrinkage rates east of the ice divide for the period 1870-1986, but after this period, more uniform shrinkage would suggest that they are more likely shrinking in response to thinning (cf. Rignot and others, 2003). Barcaza and others (2009) attribute faster absolute shrinkage (km^2 per annum) on western glaciers to high transient snowlines and increased ablation areas; however, this does not take into account glacier size and so results are not comparable.

Mountain glaciers and ice caps between 52°S and 54°S, including GCN and Isla Riesco, had relatively similar rates of area loss from 1986-2011 (Figs. 4e, 6). The observed shrinkage is in keeping with thinning observed

550 on outlet glaciers (Möller and others, 2007). Mountain glaciers south of 54°S and the Cordillera Darwin, Isla
551 Hoste, Tierra del Fuego and Monte Sarmiento ice caps have had respectively less change since the "LIA",
552 which agrees with the findings of other studies (e.g., Kuylenstierna and others, 1996). These glaciers shrank
553 fastest from 1986-2001 (Fig. 4e), during a period of rapid warming south of 46°S (Villalba and others, 2003).

554

555 **5. CONCLUSIONS**

556 We mapped glacier area and length for 640 Patagonian glaciers in 1870, and 626 glaciers for 1986, 2001 and
557 2011 (the remainder having entirely disappeared). The region is characterised by four large icefields and
558 numerous small glaciers. These data provide the longest term estimates (141 years) for regional glacier
559 shrinkage of which we are aware. During this time, modelling and instrumented records show increases in
560 atmospheric temperatures and reductions in precipitation. Almost all the glaciers shrank from their "LIA"
561 limit. However, it was difficult to map this limit for some glaciers, and the area lost is a minimum estimate.
562 For the first time, we have compared glacier length and area changes following the end of the "LIA" to
563 change in recent decades, and been able to compare rates of shrinkage both between icefields, but also for
564 small isolated glaciers and ice caps across the study region, from 41° to 56°S.

565 Since 1870, 90.2% of glaciers have shown continued and accelerating shrinkage. Small glaciers (> 5 km^2),
566 mountain glaciers and ice caps around icefields and outlet glaciers in particular are shrinking very rapidly.
567 We have demonstrated that mean glacier shrinkage is now faster than it was at the end of the "LIA", with
568 the NPI and SPI shrinking at approximately twice the rate from 2001-2011 as from 1870-1986. However it
569 should be noted that during the 116 years between observations, glaciers may have shrunk at rates faster or
570 slower than the mean, with periods of stagnation or advance not accounted for during this period in our
571 study.

572 The detailed analysis undertaken allows regional trends to be observed. Size, latitude and terminal
573 environment exert the largest controls on glacier shrinkage, with smaller (> 5 km^2), land-terminating,
574 northerly glaciers generally shrinking faster. For mountain glaciers north of 52°S and the NPI and the SPI, the
575 period of fastest shrinkage was 2001-2011. Glaciers in the Chilean Lake District and ice caps on volcanic
576 mountains north of 46°S (which also have high mean elevations), and small mountain glaciers east of the SPI
577 had the fastest area loss rates, with accelerating shrinkage after 2001. Annual rates of area loss for mountain
578 glaciers and ice caps north of 52°S are faster than the outlet glaciers of the NPI and the SPI, which may be
579 because they are smaller.

580 There is considerable inter-catchment variability, with glaciers (particularly lacustrine and marine-
581 terminating glaciers) responding non-linearly to external forcings, and with shrinkage being regulating by
582 calving processes and bedrock topography. Only two glaciers advanced beyond their "LIA" limits (which may

583 be because of mapping difficulties), but several glaciers advanced from 1986-2001 and 2001-2011. There is
584 evidence for only very slight asynchronous shrinkage either side of the ice divide for the NPI and SPI. Calving
585 outlet glaciers of the NPI and SPI are thinning and shrinking, but more slowly than land-terminating glaciers,
586 and are controlled more by dynamic calving processes.

587 For GCN, Isla Riesco ice caps and small (> 5 km^2) mountain glaciers between 52°S and 54°S, rates of area loss
588 accelerated after 1986 and then remained stable, with similar rates of area loss from 2001-2011, and with
589 many glaciers having no observable change. Mountain glaciers around GCN shrank fastest from 2001-2011.
590 For the Cordillera Darwin, Isla Hoste and Monte Sarmiento ice caps and glaciers south of 54°S, the period of
591 fastest area loss was 1986-2001, with rates of area loss since declining, and increasing numbers of glaciers
592 remained stable after 2001. There are clear differences in response between different regions, tidewater
593 and land-terminating glaciers.

594

595 **ACKNOWLEDGEMENTS**

596 We acknowledge Masamu Aniya for kindly providing the shapefiles of the 1975 extent of the Northern
597 Patagonian Icefield. Landsat images were provided free of charge to Neil Glasser from NASA. This work was
598 funded by a Natural Environment Research Council (NERC) grant through the Antarctic Funding Initiative
599 (grant AFI 9-01; NE/F012942/1). We gratefully acknowledge constructive and thoughtful reviews from Frank
600 Paul and Masamu Aniya.

601

602 **REFERENCES**

603 Aniya, M., 1988. Glacier inventory for the Northern Patagonian Icefield, Chile, and variations 1944/45 to
604 1985/86. *Arctic Alpine Res.,* **20**(2), 179-187.

605 Aniya, M., 1995. Holocene Glacial Chronology in Patagonia: Tyndall and Upsala Glaciers. *Arctic Alpine Res.,*
606 **27**, 311-322.

607 Aniya, M., 1996. Holocene variations of Ameghino Glacier, southern Patagonia. *Holocene,* **6**(2), 247-252.

608 Aniya, M., 1999. Recent Glacier Variations of the Hielos Patagónicos, South America, and Their Contribution
609 to Sea-Level Change. *Arctic, Antarct, Alpine Res.,* **31**(2), 165-173.

610 Aniya, M., 2001. Glacier variations of Hielo Patagónico Norte, Chilean Patagonia, since 1944/45, with special
611 reference to variations between 1995/96 and 1999/2000. *Bull. Glaciol. Res.,* **18**, 55-63.

612 Aniya, M., 2007. Glacier variations of Hielo Patagónico Norte, Chile, for 1944/45-2004/05. *Bull. Glaciol. Res.,*
613 **24**, 59-70.

614 Aniya, M., Naruse, R., Shizukuishi, M., Skvarca, P. and Cassassa, G., 1992. Monitoring recent glacier variations
615 in the Southern Patagonian Icefield, utilizing remote sensing data. In Fritz, L. and Lucas, J., editors, *Int.*
616 *Archive Photogrammetry Remote Sens.*, Washington, Committee of the XVII International Congress for
617 Photogrammetry and Remote Sensing.

618 Aniya, M., Sato, H., Naruse, R., Skvarca, P. and Cassassa, G., 1996. The use of satellite and airborne imagery
619 to inventory outlet glaciers of Southern Patagonian Icefield, South America. *Photogrammetric*
620 *Engineering Remote Sens.,* **62**(12), 1361-1369.

621 Aniya, M., Sato, H., Naruse, R., Skvarca, P. and Casassa, G., 1997. Recent Glacier Variations in the Southern
622 Patagonia Icefield, South America. *Arctic Alpine Res.,* **29**(1), 1-12.

623 Araneda, A., Torrejón, F., Aguayo, M., Torres, L., Cruces, F., Cisternas, M. and Urrutia, R., 2007. Historical
624 records of San Rafael glacier advances (North Patagonian Icefield): another clue to 'Little Ice Age'
625 timing in southern Chile? *Holocene,* **17**(7), 987-998.

626 Aravena, J.-C. and Luckman, B.H., 2009. Spatio-temporal rainfall patterns in Southern South America.
627 *Internat. J. Climat.,* **29**(14), 2106-2120.

628 Arendt, A.A., Echelmeyer, K.A., Harrison, W.D., Lingle, C.S. and Valentine, V.B., 2002. Rapid wastage of Alaska
629 glaciers and their contribution to rising sea level. *Science,* **297**(5580), 382-386.

630 Barcaza, G., Aniya, M., Matsumoto, T., and Aoki, T., 2009. Satellite-derived equilibrium lines in Northern
631 Patagonian Icefield, Chile, and their implications to glacier variations. *Arctic, Antarctic and Alpine*
632 *Research,* **41**(2), 174-182.

633 Bolch, T., Menounos, B. and Wheate, R., 2010. Landsat-based inventory of glaciers in western Canada, 1985-
634 2005. *Remote Sens. Environ.,* **114**(1), 127-137.

635 Bown, F. and Rivera, A., 2007. Climate changes and recent glacier behaviour in the Chilean Lake District.
636 *Global Planet. Change,* **59**(1-4), 79-86.

637 Braithwaite, R.J. and Raper, S.C.B., 2002. Glaciers and their contribution to sea level change. *Physics and*
638 *Chemistry of the Earth, Parts A/B/C,* **27**, 1445-1454.

639 Buttstädt, M., Möller, M., Iturraspe, R., and Schneider, C., 2009. Mass balance evolution of Martial Este
640 Glacier, Tierra del Fuego (Argentina) for the period 1960–2099. *Adv. Geosci.* **22**, 117-124.

641 Carrasco, J.F., Osorio, R., and Casassa, G., 2008. Secular trend of the equilibrium-line altitude on the western
642 side of the southern Andes, derived from radiosonde and surface observations. *J. Glaciol.* **54**(186),
643 538-550.

644 Casassa, G., Smith, K., Rivera, A., Araos, J., Schnirch, M., and Schneider, C., 2002. Inventory of glaciers in isla
645 Riesco, Patagonia, Chile, based on aerial photography and satellite imagery. *Ann. of Glaciol.* **34**, 373-
646 378.

647 Chen, J.L., Wilson, C.R., Tapley, B.D., Blankenship, D. and Ivins, E.R., 2007. Patagonia icefield melting
648 observed by Gravity Recovery and Climate Experiment (GRACE). *Geophys. Res. Lett.,* **34**(22), L22501.

649 Church, J.A., Gregory, J.M., Huybrechts, P., Kuhn, M., Lambeck, K., Nhuan, M.T., and Woodworth, P.L., 2001.
650 Changes in sea level. In: Houghton, J.T., Ding, Y., Griggs, D.J., Noguer, M., van der Linden, P.J., Dai, X.,
651 Maskell, K., and Johnson, C.A. *Climate Change 2001: The Physical Science Basis. Contribution of*
652 *Working Group I to the Third Assessment Report of the Intergovernmental Panel on Climate Change.*
653 Cambridge University Press, p. 639-694.

654 Cook, A.J., Fox, A.J., Vaughan, D.G. and Ferrigno, J.G., 2005. Retreating glacier fronts on the Antarctic
655 Peninsula over the past half-century. *Science,* **308**(5721), 541-544.

656 Davies, B.J., Carrivick, J.L., Glasser, N.F., Hambrey, M.J. and Smellie, J.L., 2011. A new glacier inventory for
657 2009 reveals spatial and temporal variability in glacier response to atmospheric warming in the
658 northern Antarctic Peninsula, 1988-2009. *Cryosphere Discuss,* **5**, 3541-3595.

659 Evans, I.S., 2006. Local aspect asymmetry of mountain glaciation: A global survey of consistency of favoured
660 directions for glacier numbers and altitudes. *Geomorphology,* **73**(1-2), 166-184.

661 Farr, T.G., Rosen, P.A., Caro, E., Crippen, R., Duren, R., Hensley, S., Kobrick, M., Paller, M., Rodriguez, E., Roth,
662 L., Seal, D., Shaffer, S., Shimada, J., Umland, J., Werner, M., Oskin, M., Burbank, D., and Alsdorf, D.,
663 2007. The Shuttle Radar Topography Mission. *Reviews in Geophysics,* **45**(2), 1-33.

664 Frey, H., and Paul, F., 2012. On the suitability of the SRTM DEM and ASTER GDEM for the compilation of
665 topographic parameters in glacier inventories. *Internat. J. of Applied Earth Observation and*
666 *Geoinformation,* **18**, 480-490.

667 Garreaud, R.D., Vuille, M., Compagnucci, R. and Marengo, J., 2009. Present-day South American climate.
668 *Palaeogeog., Palaeoclimat., Palaeoecol.,* **281**(3-4), 180-195.

669 Giese, B., Urizr, C., Fuckar, S., 2002. Southern Hemisphere origins of the 1976 climatic shift. *Geophys. Res.*
670 *Lett.*, **29**(2). Doi: 10.1029/2001GL013268.

671 Glasser, N.F., Hambrey, M.J. and Aniya, M., 2002. An advance of Soler Glacier, North Patagonian Icefield, at
672 c. AD 1222-1342. *Holocene,* **12**(1), 113-120.

673 Glasser, N.F., Harrison, S., Jansson, K.N., Anderson, K. and Cowley, A., 2011. Global sea-level contribution
674 from the Patagonian Icefields since the Little Ice Age maximum. *Nature Geosci.,* **4**(5), 303-307.

675 Glasser, N.F., Harrison, S., Winchester, V. and Aniya, M., 2004. Late Pleistocene and Holocene palaeoclimate
676 and glacier fluctuations in Patagonia. *Global Planet. Change,* **43**(1-2), 79-101.

677 Glasser, N.F., Jansson, K.N., Harrison, S., and Kleman, J., 2008. The glacial geomorphology and Pleistocene
678 history of South America between 38°S and 56°S. *Quat. Sci. Rev*., **27**, 365-390.

679 Glasser, N.F., Jansson, K.N., Harrison, S. and Rivera, A., 2005. Geomorphological evidence for variations of
680 the North Patagonian Icefield during the Holocene. *Geomorphology,* **71**, 263-277.

681 Glasser, N.F., and Scambos, T.A., 2008. A structural glaciological analysis of the 2002 Larsen B ice shelf
682 collapse. *J. Glacio.* **54**(184), 3-16.

683 Granshaw, F.D. and Fountain, A.G., 2006. Glacier change (1958-1998) in the North Cascades National Park
684 Complex, Washington, USA. *J. Glacio.,* **52**, 251-256.

685 Harrison, S,. Glasser, N.F., Duller, G.A.T., and Jansson, K.N., 2012. Early and mid-Holocene age for the
686 Tempanos moraines, Laguna San Rafael, Patagonian Chile. *Quat. Sci. Rev.***, 31**(0), 82-92.

687 Harrison, S. and Winchester, V., 2000. Nineteenth- and Twentieth-Century Glacier Fluctuations and Climatic
688 Implications in the Arco and Colonia Valleys, Hielo Patagónico Norte, Chile. *Arctic, Antarctic, and*
689 *Alpine Research,* **32**(1), 55-63.

690 Harrison, S., Winchester, V. and Glasser, N., 2007. The timing and nature of recession of outlet glaciers of
691 Hielo Patagónico Norte, Chile, from their Neoglacial IV (Little Ice Age) maximum positions. *Global*
692 *Planet. Change,* **59**(1-4), 67-78.

693 Hijmans, R. J., Cameron, S. E., Parra, J. L., Jones, P. G., Jarvis, A., 2005. Very high resolution interpolated
694 climate surfaces for global land areas. *Int. J. Climatol.,* **25**, 1965-1978.

695 Hock, R., de Woul, M. Radíc, V., and Dyurgeriv, M., 2009. Mountain glaciers and ice caps around Antarctica
696 make a large sea-level rise contribution. *Geophys. Res. Lett.,* **36**, L07501, 1-5.

697 Holmlund, P., and Fuenzalida, H., 1995. Anomalous glacier responses to 20th century climatic changes in
698 Darwin Cordillera, southern Chile. *J. Glaciol.*, **41**(139), 465-473.

699 Ivins, E.R., Watkins, M.M., Yuan, D.-N., Dietricj, R., Casassa, G., and Rülke, A., 2011. On-land ice loss and
700 glacial isostatic adjustment at the Drake Passage: 2003-2009. *J. Geophys. Res.* **116**, B02403.

701 Jarvis, A., Reuter, H.I., Nelson, A., Guevaram E., 2008. Hole-filled seamless SRTM data V4. *International*
702 *Centre for Tropical Agriculture (CIAT)*, available from http://srtm.csi.cgiar.org.

703 Jiskoot, H., Curran, C.J., Tessler, D.L. and Shenton, L.R., 2009. Changes in Clemenceau Icefield and Chaba
704 Group glaciers, Canada, related to hypsometry, tributary detachment, length-slope and area-aspect
705 relations. *Ann. Glaciol.*, **50**(53), 133-143.

706 Koch, J. and Kilian, R., 2005. 'Little Ice Age' glacier fluctuations, Gran Campo Nevado, southernmost Chile.
707 *Holocene,* **15**(1), 20-28.

708 Koppes, M., Conway, H., Rasmussen, L.A., and Chernos, M., 2011. Deriving mass balance and calving
709 variations from reanalysis data and sparse observations, Glaciar San Rafael, northern Patagonia, 1950-
710 2005. *The Cryosphere*, **5**, 791-808.

711 Kuylenstierna, J.L., Rosqvist, G.C. and Holmund, P., 1996. Late-Holocene glacier variations in the Cordillera
712 Darwin, Tierra del Fuego, Chile. *Holocene,* **6**(3), 353-358.

713 Lopez, P., Chevallier, P., Favier, V., Pouyaud, B., Ordenes, F. and Oerlemans, J., 2010. A regional view of
714 fluctuations in glacier length in southern South America. *Global Planet. Change,* **71**(1-2), 85-108.

715 Masiokas, M.H., Luckman, B.H., Villalba, R., Delgado, S., Skvarca, P. and Ripalta, A., 2009a. Little Ice Age
716 fluctuations of small glaciers in the Monte Fitz Roy and Lago del Desierto areas, south Patagonian
717 Andes, Argentina. *Palaeogeog., Palaeoclimat., Palaeoecol.,* **281**, 351-362.

718 Masiokas, M.H., Rivera, A., Espizua, L.E., Villalba, R., Delgado, S., and Aravena, J.C., 2009b. Glacier
719 fluctuations in extratropical South America during the past 1000 years. *Palaogeog. Palaeoclim.*
720 *Palaeoecol.* **281**, 242-268.

721 Masiokas, M.H., Villalba, R., Luckman, B.H., Lascano, M.E., Delgado, S. and Stepanek, P., 2008. 20th-century
722 glacier recession and regional hydroclimatic changes in northwestern Patagonia. *Global Planet.*
723 *Change,* **60**(1-2), 85-100.

724 Meier, M.F., Dyurgerov, M.B. and McCabe, G.J., 2003. The health of glaciers: Recent changes in glacier
725 regime. *Climatic Change,* **59**(1-2), 123-135.

726 Meier, M.F., Dyurgerov, M.B., Rick, U.K., O'Neel, S., Pfeffer, W.T., Anderson, R.S., Anderson, S.P. and
727 Glazovsky, A.F., 2007. Glaciers Dominate Eustatic Sea-Level Rise in the 21st Century. *Science*, **317**
728 (5841), 1064-1067.

729 Michel, R., and Rignot, E., 1999. Flow of Glaciar Moreno, Argentina, from repeat-pass Shuttle Imaging Radar:
730 comparison of the phase correlation method with radar interferometry. *J. Glaciol.* **45**, 93-100.

731 Möller, M. and Schneider, C., 2008. Climate sensitivity and mass-balance evolution of Gran Campo Nevado
732 ice cap, southwest Patagonia. *Ann. Glaciol.*, **48**(1), 32-42.

733 Möller, M., Schneider, C., and Kilian, R., 2007. Glacier change and climate forcing in recent decades at Gran
734 Campo Nevado, southernmost Patagonia. *Ann. Glaciol.,* **46**(1), 136-144.

735 Montecinos, A., and Aceituno, P., 2003. Seasonality of the ENSO-related rainfall variability in Central Chile
736 and associated circulation anomalies. *J. Climate,* **16**(2), 281-196.

737 Naruse, R. and Skvarca, P., 2000. Dynamic Features of Thinning and Retreating Glaciar Upsala, a Lacustrine
738 Calving Glacier in Southern Patagonia. *Arctic, Antarct., Alpine Res.,* **32**, 485-491.

739 Naruse, R., Skvarca, P. and Takeuchi, Y., 1997. Thinning and retreat of Glaciar Upsala, and an estimate of
740 annual ablation changes in southern Patagonia. *Ann. Glaciol.,* **24**, 38-42.

741 Oerlemans, J. and Fortuin, J.P.F., 1992. Sensitivity of glaciers and small ice caps to greenhouse warming.
742 *Science,* **258**(5079), 115-117.

743 Paul, F., 2002. Changes in glacier area in Tyrol, Austria, between 1969 and 1992 derived from Landsat 5
744 Thematic Mapper and Austrian glacier inventory data. *Int. J. Remote Sensing***, 23**(4), 787-799.

745 Paul, F., Barry, R.G., Cogley, J.G., Frey, H., Haeberli, W., Ohmura, A., Ommanney, C.S.L., Raup, B., Rivera, A.
746 and Zemp, M., 2009. Recommendations for the compilation of glacier inventory data from digital
747 sources. *Ann. Glaciol.,* **50**(53), 119-126.

748 Racoviteanu, A.E., Paul, F., Raup, B., Khalsa, S.J.S. and Armstrong, R., 2009. Challenges and recommendations
749 in mapping of glacier parameters from space: results of the 2008 Global Land Ice Measurements from
750 Space (GLIMS) workshop, Boulder, Colorado, USA. *Ann. Glaciol.,* **50**(53), 53-69.

751 Ramirez, E., Francou, B., Ribstein, P., Descloitres, M., Guerin, R., Mendoza, J., Gallaire, R., Pouyaud, B. and
752 Jordan, E., 2001. Small glaciers disappearing in the tropical Andes: a case-study in Bolivia: Glaciar
753 Chacaltaya (16 degrees S). *J. Glaciol.,* **47**(157), 187-194.

754 Raper, S.C.B. and Braithwaite, R.J., 2009. Glacier volume response times and its links to climate and
755 topography based on a conceptual model of glacier hypsometry. *The Cryosphere*, 3, 183-194.

756 Rau, F., Mauz, F., Vogt, S., Khalsa, S.J.S. and Raup, B., 2005. *Illustrated GLIMS Glacier Classification Manual,*
757 *Version 1.0*. GLIMS Regional Centre, 'Antarctic Peninsula', GLIMS (Global Land Ice Measurement from
758 Space), NSIDC, 36 pp.

759 Raup, B. and Khalsa, S.J.S., 2010. *GLIMS Analysis Tutorial*. www.GLIMS.org, GLIMS, Global Land Ice
760 Measurements from Space, NSIDC, 15 pp.

761 Raup, B., Kääb, A., Kargel, J.S., Bishop, M.P., Hamilton, G., Lee, E., Paul, F., Rau, F., Soltesz, D., Khalsa, S.J.S.,
762 Beedle, M. and Helm, C., 2007a. Remote sensing and GIS technology in the Global Land Ice
763 Measurements from Space (GLIMS) Project. *Computers and Geosciences,* **33**(1), 104-125.

764 Raup, B., Racoviteanu, A., Khalsa, S.J.S., Helm, C., Armstrong, R. and Arnaud, Y., 2007b. The GLIMS geospatial
765 glacier database: A new tool for studying glacier change. *Global Planet. Change,* **56**(1-2), 101-110.

766 Reuter, H.I., Nelson, A., and Jarvis, A., 2007. An evaluation of void filling interpolation methods for SRTM
767 data. *Internat. J. of Geographic Information Science***, 21**, 983-1008.

768 Rignot, E., Rivera, A. and Casassa, G., 2003. Contribution of the Patagonia Icefields of South America to Sea
769 Level Rise. *Science,* **302**(5644), 434-437.

770 Rivera, A. and Casassa, G., 1999. Volume changes on Pio XI glacier, Patagonia: 1975–1995. *Global Planet.*
771 *Change,* **22**(1-4), 233-244.

772 Rivera, A. and Cassassa, G., 2004. Ice elevation, areal and frontal changes of glaciers from National Park
773 Torres del Paine, Southern Patagonian Icefield. *Arctic, Antarct. Alpine Res.,* **36**(4), 379-389.

774 Rivera, A., Benham, T., Casassa, G., Bamber, J. and Dowdeswell, J.A., 2007. Ice elevation and areal changes of
775 glaciers from the Northern Patagonia Icefield, Chile. *Global Planet. Change,* **59**, 126-137.

776 Rivera, A., Bown, F., Carrión, D., and Zenteno, P., 2012. Glacier responses to recent volcanic activity in
777 Southern Chile. *Env. Res. Lett.* **7**, 1-10.

778 Rivera, A., Bown, F., Casassa, G.,Acuña, C., and Clavero, J., 2005. Glacier shrinkage and negative mass
779 balance in the Chilean Lake District (40°S). *Hydrological Sciences,* **50**(6), 963-974.

780 Rivera, A., Casassa, G., Bamber, J. and Kääb, A., 2005. Ice-elevation changes of Glaciar Chico, southern
781 Patagonia, using ASTER DEMs, aerial photographs and GPS data. *J. Glaciol.,* **51**(172), 105-112.

782 Rivera, A., Koppes, M., Bravo, C., and Aravena, J.C., 2011. Little Ice Age advance and retreat of Glaciar Jorge
783 Montt, Chilean Patagonia, recorded in maps, air photographs and dendrochronology. *Clim. Past.*
784 *Discsuss***, 7**, 3131-3164.

785 Rott, H., Stuefer, M., Siegel, A., Skvarca, P., and Eckstaller, A., 1998. Mass fluxes and dynamics of Moreno
786 Glacier, Southern Patagonian Icefield. *Geophys. Res. Lett.,* **25**(9), 1407-1410.

787 Sagredo, E.A., and Lowell, T.V., 2012. Climatology of Andean glaciers: a framework to understand glacier
788 response to climate change. *Global Planet. Change.* **86-87**, 101-109.

789 Scherler, D., Bookhagen, B., and Strecker, M.R., 2011. Spatially variable response of Himalayan glaciers to
790 climate change affected by debris cover. *Nature Geosci.* **4**(3), 156-159.

791 Schneider, C., Schnirch, M., Acuña, C., Casassa, G. and Kilian, R., 2007. Glacier inventory of the Gran Campo
792 Nevado Ice Cap in the Southern Andes and glacier changes observed during recent decades. *Global*
793 *Planet. Change,* **59**(1-4), 87-100.

794 Stokes, C.R,. Popovnin, V., Aleynikov, A., Gurney, S.D,. and Shahgedanova, M., 2007. Recent glacier retreat in
795 the Caucasus Mountains, Russia, and associated increase in supraglacial debris cover and supra-
796 /proglacial lake development. *Ann. Glaciol.* **46**, 195-203.

797 Stueffer, M., Rott, H., and Skvarca, R., 2007. Glaciar Perito Moreno, Patagonia: climate sensitivities and
798 glacier characteristics preceding the 2003/04 and 2005/06 damming events. *J. Glaciol.***, 53**(180), 3-16.

799 Svoboda, F. and Paul, F., 2009. A new glacier inventory on southern Baffin Island, Canada, from ASTER data:
800 I. Applied methods, challenges and solutions. *Ann. Glaciol.,* **50**(53), 11-21.

801 Tucker, C.J., Grant, D.M. and Dykstra, J.D., 2004. NASA's global orthorectified LANDSAT data set.
802 *Photogrammetric Engineering and Remote Sensing,* **70**, 313-322.

803 Vaughan, D.G., Marshall, G.J., Connelly, W.M., King, J.C. and Mulvaney, R., 2001. Devil in the detail. *Science,*
804 **293**(5536), 1777-1779.

805 Villalba, R., 1994. Tree-ring and glacial evidence for the medieval warm epoch and the Little Ice Age in
806 southern South America. *Climatic Change,* **26**, 183-197.

807 Villalba, R., Lara, A., Boninsegna, J.A., Masiokas, M., Delgado, S., Aravena, J.C., Roig, F.A., Schmelter, A.,
808 Wolodarsky, A. and Ripalta, A., 2003. Large-Scale Temperature Changes across the Southern Andes:
809 20th-Century Variations in the Context of the Past 400 Years. *Climatic Change,* **59**(1-2), 177-232.

810 Warren, C.R., and Aniya, M., 1999. The calving glaciers of southern South America. *Global Planet. Change,*
811 **22**(1-4), 59-77.

812 Warren, C.R., Glasser, N.F., Kerr, A., Harrison, S., WInchester, V,. and Rivera, A., 1995. Characteristics of
813 tidewater glacier calving at Glaciar San Rafael, Chile. *J. Glaciol.,* **41**, 273-289.

814 Willis, M.J., Melkonian, A.K., Pritchard, M.E. and Ramage, J.M., 2011. Ice loss rates at the Northern
815 Patagonian Icefield derived using a decade of satellite remote sensing. *Remote Sens. Environ.*, **117**(0),
816 184-198.

817 Winchester, V. and Harrison, S., 1996. Recent Oscillations of the San Quintin and San Rafael Glaciers,
818 Patagonian Chile. *Geografiska Annaler. Series A, Physical Geography,* **78**, 35-49.

819 Winchester, V. and Harrison, S., 2000. Dendrochronology and lichenometry: colonization, growth rates and
820 dating of geomorphological events on the east side of the North Patagonian Icefield, Chile.
821 *Geomorphology,* **34**(3-4), 181-194.

822 WGMS (2008): Global Glacier Changes: facts and figures. Zemp, M., Roer, I., Kääb, A., Hoelzle, M., Paul, F.
823 and Haeberli, W. (eds.), UNEP, World Glacier Monitoring Service, Zurich, Switzerland: 88 pp.

824

825

FIGURES

Fig. 1. Location of the main icefields and glaciers in southern South America, showing abbreviations used in text and tables. The inset shows the wider location of the study area. Mean annual temperature data for the four temperature transects was obtained from Hijmans and others (2005) from a 1 km resolution raster dataset. Note decreasing temperatures over the icefields and in areas of high elevation. Local variations reflect the influence of fjords, rivers and mountains. Precipitation data for stations where there were records longer than 10 years was obtained from the Dirección Meteorológica de Chile. Note the strong west to east precipitation gradients that exist across the study area and the low number of stations; precipitation values at each glacier are therefore uncertain. Lakes larger than 15 km^2 are shown.

Fig. 2. Examples of glacier change for parts of the NPI. Note the trimlines and mapped moraines, which were used to reconstruct maximum glacier extent during the "LIA" (AD 1870). Dashed black lines illustrate mapped glacier lengths for 2011; previous years follow the same flowline. (a) Overview of the NPI. (b) The snout of Glaciar San Rafael. (c) The snout of Glaciar San Quintin. In this case, because of well-documented evidence, the outermost moraines were used in the definition of the "LIA". (d) The northern NPI, including NPI-1 (Glaciar Grosse). (e) Landsat ETM+ image for 2001, with clearly defined trimlines and moraines demarking the "LIA" extent (dashed white outline).

Fig. 3. (a) Glacierised area in 2011 and number of glaciers in each size class. (b) Glacier aspect for the main regions. (c) Number of glaciers in each 'Primary Classification' (from GLIMS protocols). (d) Numbers of glaciers in each category of the 'Form' attribute (from GLIMS protocols). (e) Mean altitude for glaciers across the study region. (f) Comparison between glacier area in 2001 and glacier maximum altitude, with regression line. Note logarithmic scale. (g) Relationship between glacier latitude and median altitude. (h) Relationship between glacier length and mean slope. Note logarithmic scale.

Fig. 4. (a) Glacierised area and rates of area loss for the NPI and SPI, with calving and land-terminating glaciers shown separately. (b) Rate of change 2001-2011 against latitude, with glaciers divided into size classes. (c) Rate of glacier shrinkage 2001-2011 (per cent per annum) against glacier mean altitude, with glaciers divided into size classes. (d) Rate of glacier shrinkage 2001-2011 (per cent per annum) against glacier mean slope, with glaciers divided into size classes.(e) Rate of change (% a^{-1}) for each region over three time periods. For El Condor and Southern Patagonian Mountain Glaciers (starred), the anomalously high shrinkage rates are given on the figure. See Table 2 for abbreviations.

Fig. 5. Rate of annual change (% a^{-1}) for 2001-2011 against 2011 glacier size for each region. SPMG refers to isolated glaciers surrounding the SPI. "National Parks" includes Parque Nacional Vicente Perez Rosales, Parque Nacional Corcovado and Parque Nacional Quelat. Grey circles denote calving glaciers; black squares

858 denote land-terminating glaciers. Solid horizontal line is nil change; shrinkage is below this line, and advance
859 is above. Latitude of regional centre is shown.

860 **Fig. 6.** Graphs showing cumulative length changes for selected glaciers for key icefields. The black line
861 indicates a glacier that terminates on land. The grey line with short dashes indicates lacustrine-terminating
862 glaciers. The thick black dashed line indicates marine-terminating (tidewater) glaciers. (a) Cerro Erasmo, (b)
863 Northern Patagonian Icefield, (c) El Volcan, (d) Southern Patagonian Icefield, (e) Gran Campo Nevado, (f)
864 Cordillera Darwin.

865 **Fig. 7.** Map of key icefields showing overall glacier shrinkage, 1870-2011. Glacier extent in 1870 is shown in
866 white. Lakes larger than 15 km^2 are also shown.

867 **Fig.8.** Map of key icefields, illustrating period of fastest shrinkage. Glaciers in dark grey shrank fastest
868 between 2001-2011, mid-grey between 1986-2001, light-grey, 1975-1986 (data for the NPI only), and white,
869 1870-1986. Glaciers with cross-hatching advanced and glaciers with stipples did not change. Glacier outlines
870 are from 2011. Lakes larger than 15 km^2 are also shown.

871

872 **TABLES**

873 **Table 1.** Identification of glaciological and geomorphological features. After Glasser and others, 2005, 2008.

Landform / feature	**Identification criteria**		**Possible errors**	**Glaciological significance**
	Morphology	**Colour/structure/texture**		
Contemporary glaciers	Bare ice, snow and debris, surface structures (crevasses, longitudinal structures, folds, lakes and supraglacial streams).	White to blue, smooth to rough surface. Abrupt transition.	Overestimate where snout is covered in snow. Underestimate where snout is covered with debris.	Foci for ice discharge
Ice divides	Where ice divides have not previously been published (e.g. on GLIMS), they are identified through mapping high points, cols, topographic divides, glaciological structures such as crevasses and longitudinal surface structures (see Glasser and Scambos, 2008). Previously published ice divides are used for the NPI, SPI, Cordillera Darwin and Gran Campo Nevado (see GLIMS).		Error is likely to be highest in flat summits. Interpreter error in ice divide mapping is likely to be the largest source of error. Limited by the lack of a DEM that is well resolved over the ice.	No migration of ice divides is assumed for calculation of glacier change.
Debris-covered snout	There may be arcuate or linear glaciological structures, ponds or bare ice visible. Where the glacier terminates in a lake, a fragmented floating margin may be visible.	Dark brown. Sharp transition to vegetation. Surface is rough and pitted.	Supraglacial debris cover on snout may be confused with lateral or terminal moraines; similar spectral properties to rock valley sides.	Denotes glacier extent. May indicate downwasting.
Trimlines	Sub-horizontal lines on valley sides separating areas of vegetated and non-vegetated land or areas with different types of vegetation.	Sharp altitudinal change in surface colour and texture as a result of changes in vegetation cover.	Possible but unlikely; confusion with sub-horizontal features as lake shorelines	Former vertical extent of glaciers.
Terminal moraines	Prominent cross-valley single or multiple ridges with positive relief. Linear, curved, sinuous or saw-toothed plan.	Shadowing due to change in relief and change in colour when moraines are vegetated.	Possible, but unlikely, confusion with trimlines where moraines have a low relative height.	Mark the former terminal position of outlet glaciers. Innermost moraine is taken as the "LIA" limit except where this has been published elsewhere.
Cirques	Large amphitheatre-shaped hollows on mountain flanks or incised into plateau edges. Sharp boundaries with surrounding terrain.	Shadowing due to change in height or relative relief. Cirque floors may be different in colour to surrounding land.	Possible, but unlikely, confusion with mass-movement or landslip scars, particularly beneath volcanic plateau.	Indicates presents of localised or restricted mountain glaciation.

874

875 **Table 2.** Summary of the glacier inventory, divided into regions (region codes given in brackets). Regions are ordered north to south.

Region	Region code	Latitude	Longitude	Largest glacier in 2011 (km^2)	Smallest glacier in 2011 (km^2)	Mean topographic data in 2000		Number of glaciers		Glacierised area (km^2)			
						Elevation (m a.s.l.)	Slope (degrees)	1870	1986-2011	1870	1986	2001	2011
Parque Nacional Vicente Perez Rosales	VPR	-41.15	-71.88	65.8	65.8	2158	23	1	1	89.4	72.1	71.2	65.8
Hornopiren	H	-41.99	-72.19	32	1.4	1614	20	8	8	146.4	113.1	104.3	96.1
Parque Nacionale Corcovado	PNC	-43.49	-72.5	82	0.4	1492	23	16	16	453.4	330.4	311.7	284.1
Parque Nacional Queulat	PNQ	-44.40	-72.42	101.7	1.5	1446	18	5	5	265.4	220.9	213.4	212.4
Cerro Hudson	CH	-46.08	-72.93	22.3	0.9	1405	18	10	9	268.6	232.0	229.7	221.9
Cerro Erasmo	CE	-46.16	-73.2	40.4	2.9	1375	21	7	7	181.2	151.5	144.1	141.0
Northern Patagonian Icefield	NPI	-47.01	-73.5	781.7	1.0	1340	20	44	44	4635.7	4142.3	4070.2	3976.0
Northern Patagonian Mountain Glaciers	NPMG	-47.01	-73.50	27.6	0.2	1471	22	25	25	251.0	186.3	178.3	176.1
Cordon la Parvas	CLP	-46.59	-73.05	16.3	0.7	1483	27	16	16	125.8	93.7	88.4	85.6
Cordillera Lago General Carrera	CLGC	-46.83	-73.07	33.0	1.4	1671	28	18	18	189.8	138.6	133.2	131.6
El Volcan	EV	-47.59	-72.61	48.2	0.7	1521	21	40	36	511.8	387.1	361.9	354.3
Monte San Lorenzo	MSL	-47.59	-72.37	48.7	2.6	1948	27	11	10	207.8	150.3	145.4	142.9
Lago del Desierto	LDP	-48.83	-73.20	192.4	7.1	1579	23	7	6	363.7	294.2	290.3	271.3
El Condor	EC	-49.11	-72.80	74.1	3.0	1403	22	2	2	137.8	137.8	137.8	77.1
Cerro Paine Grande	CPG	-50.90	-73.20	22.2	1.5	1313	26	13	13	96.4	77.9	76.5	76.4
Southern Patagonian Icefield	SPI	-49.74	-73.47	1343.9	0.2	1191	21	161	154	14862.1	13657.3	13424.0	13218.8
Southern Patagonian Mountain Glaciers	SPMG	-49.74	-73.47	30.4	0.5	956	26	25	25	495.4	125.1	124.7	95.2
Torres del Paine	TDP	-51.42	-73.14	11	0.5	1093	25	5	5	70.0	28.0	27.0	26.8
Monte Burney	MB	-52.32	-73.36	15.5	15.5	883	27	1	1	22.4	16.3	15.7	15.5
Gran Campo Nevado Mountain Glaciers	GCMG	-52.95	-72.99	7.2	0.1	801	22	17	17	29.4	27.0	26.4	25.3
Gran Campo Nevado	GCN	-52.95	-72.99	30.9	0.7	836	23	35	35	263.2	251.1	242.6	236.9
Isla Riesco	RI	-52.95	-72.58	35.1	7.4	858	17	4	4	120.4	110.4	107.0	106.6
Estrecho de Magallanes	M	-53.79	-72.58	180.5	180.5	717	14	1	1	187.9	183.4	182.1	180.5
Tierra del Fuego	TDF	-54.43	-70.81	76.2	3.8	748	17	4	4	173.5	168.2	164.5	163.9
Monte Sarmiento	MS	-54.57	-70.47	25	1.4	867	20	17	17	199.3	186.6	183.1	183.1
Cordillera Darwin	CD	-54.66	-69.72	160.1	0.5	938	22	94	94	2138.1	1930.2	1855.2	1832.7
Cordillera Darwin Mountain Glaciers	CDMG	-54.66	-69.72	10.4	0.4	801	21	30	30	119.3	102.8	99.0	98.9
Isla Hoste	IH	-55.22	-69.6	93.3	0.5	727	19	18	18	243.5	228.8	221.5	220.8
Entire region	**All**	**-48.58**	**-73.45**	**1343.9**	**0.14**	**1172**	**22**	**640**	**626**	**26848.8**	**23743.1**	**23229.0**	**22717.5**

876

877 **Table 3.** Glacier change for the NPI and SPI.

	Ice divide	Number of glaciers	Glacierised area 2011 (km^2)	% Change 1870-1986	% Change 1986-2001	% Change 2001-2011	Rate of change (% a^{-1}) 1870-1986	Rate of change (% a^{-1}) 1986-2001	Rate of change (% a^{-1}) 2001-2011
NPI	West	19	2962.5	-8.8	-1.9	-2.4	-0.08%	-0.12%	-0.24%
NPI	East	25	1013.5	-15.5	-1.4	-2.2	-0.13%	-0.09%	-0.22%
SPI	West	73	8417.4	-5.9	-1.9	-1.4	-0.05%	-0.13%	-0.14%
SPI	East	81	4801.4	-11.0	-1.3	-1.8	-0.09%	-0.09%	-0.18%

878

879

880 **Table 4.** Area change, percentage change and annual rates of change in each region and time period. "N" refers to the number of glaciers shrinking fastest
881 in this period. *Note for the NPI, that 20 glaciers shrank fastest between 1975-1986.

	1870-2011				1870-1986					1986-2001					2001-2011				
	Area change (km^2)	% Area change	Rate of change (km^2 a^{-1})	Rate of change (% a^{-1})	Area change (km^2)	% Area change	Rate of change (km^2 a^{-1})	Rate of change (% a^{-1})	N.	Area change (km^2)	% Area change	Rate of change (km^2 a^{-1})	Rate of change (% a^{-1})	N.	Area change (km^2)	% Area change	Rate of change (km^2 a^{-1})	Rate of change (% a^{-1})	N.
VPR	-23.6	-26.3%	-0.1	-0.19%	-17.3	-19.3%	-0.1	-0.17%	0	-1.0	-1.3%	-0.1	-0.09%	0	-5.3	-7.5%	-0.5	-0.75%	1
H	-50.3	-34.3%	-0.3	-0.24%	-33.3	-22.7%	-0.3	-0.20%	0	-8.8	-7.8%	-0.6	-0.52%	1	-8.1	-7.8%	-0.8	-0.78%	7
PNC	-169.3	-37.3%	-1.1	-0.26%	-123.0	-27.1%	-1.1	-0.23%	1	-18.8	-5.7%	-1.3	-0.38%	3	-27.5	-8.8%	-2.8	-0.88%	12
PNQ	-53.0	-20.0%	-0.4	-0.14%	-44.5	-16.8%	-0.4	-0.14%	1	-7.4	-3.4%	-0.5	-0.22%	4	-1.1	-0.5%	-0.1	-0.05%	0
CH	-46.7	-17.4%	-0.3	-0.12%	-36.5	-13.6%	-0.3	-0.12%	1	-2.4	-1.0%	-0.2	-0.07%	2	-7.8	-3.4%	-0.8	-0.34%	5
CE	-40.2	-22.2%	-0.3	-0.16%	-29.7	-16.4%	-0.3	-0.14%	2	-7.3	-4.8%	-0.5	-0.32%	3	-3.2	-2.2%	-0.3	-0.22%	2
NPI*	-659.7	-14.2%	-4.3	-0.10%	-493.4	-10.6%	-4.3	-0.09%	3	-72.1	-1.7%	-4.8	-0.12%	6	-94.1	-2.3%	-9.4	-0.23%	14
NPMG	-75.0	-29.9%	-0.6	-0.21%	-64.8	-25.8%	-0.6	-0.22%	13	-8.0	-4.3%	-0.5	-0.29%	8	-2.2	-1.2%	-0.2	-0.12%	4
CLP	-40.2	-31.9%	-0.3	-0.23%	-32.1	-25.6%	-0.3	-0.22%	4	-5.3	-5.6%	-0.4	-0.37%	6	-2.8	-3.1%	-0.3	-0.31%	5
CLGC	-58.2	-30.7%	-0.4	-0.22%	-51.2	-27.0%	-0.4	-0.23%	8	-5.4	-3.9%	-0.4	-0.26%	7	-1.6	-1.2%	-0.2	-0.12%	3
EV	-157.5	-30.8%	-1.1	-0.22%	-124.7	-24.4%	-1.1	-0.21%	12	-25.1	-6.5%	-1.7	-0.43%	18	-7.7	-2.1%	-0.8	-0.21%	5
MSL	-64.9	-31.2%	-0.5	-0.22%	-57.5	-27.7%	-0.5	-0.24%	3	-4.9	-3.2%	-0.3	-0.22%	5	-2.6	-1.8%	-0.3	-0.18%	2
LDP	-92.4	-25.4%	-0.6	-0.18%	-69.5	-19.1%	-0.6	-0.16%	0	-3.9	-1.3%	-0.3	-0.09%	2	-19.0	-6.5%	-1.9	-0.65%	4
EC	-60.7	-44.1%	0.0	-0.31%	0.0	0.0%	0.0	0.00%	0	0.0	0.0%	0.0	0.00%	0	-60.7	-44.1%	-6.1	-4.41%	2
CPG	-20.0	-20.7%	-0.2	-0.15%	-18.4	-19.1%	-0.2	-0.17%	4	-1.5	-1.9%	-0.1	-0.13%	4	-0.1	-0.1%	0.0	-0.01%	0
SPI	-1643.3	-11.1%	-10.4	-0.08%	-1204.8	-8.1%	-10.4	-0.07%	51	-233.3	-1.7%	-15.6	-0.11%	39	-205.2	-1.5%	-20.5	-0.15%	59
SPMG	-400.3	-80.8%	-3.2	-0.57%	-370.3	-74.7%	-3.2	-0.64%	20	-0.5	-0.4%	0.0	-0.03%	0	-29.5	-23.7%	-2.9	-2.37%	4
TDP	-43.2	-61.7%	-0.4	-0.44%	-42.0	-60.0%	-0.4	-0.52%	3	-0.9	-3.3%	-0.1	-0.22%	1	-0.3	-1.0%	0.0	-0.10%	1
MB	-7.0	-31.1%	-0.1	-0.22%	-6.2	-27.5%	-0.1	-0.24%	0	-0.6	-3.6%	0.0	-0.24%	1	-0.2	-1.4%	0.0	-0.14%	0
GCMG	-4.1	-13.9%	0.0	-0.10%	-2.3	-8.0%	0.0	-0.07%	2	-0.7	-2.5%	0.0	-0.17%	3	-1.1	-4.0%	-0.1	-0.40%	4
GCN	-26.3	-10.0%	-0.1	-0.07%	-12.1	-4.6%	-0.1	-0.04%	2	-8.5	-3.4%	-0.6	-0.23%	11	-5.6	-2.3%	-0.6	-0.23%	10
RI	-13.9	-11.5%	-0.1	-0.08%	-10.1	-8.4%	-0.1	-0.07%	0	-3.4	-3.1%	-0.2	-0.21%	3	-0.4	-0.4%	0.0	-0.04%	1
M	-7.5	-4.0%	0.0	-0.03%	-4.6	-2.4%	0.0	-0.02%	0	-1.3	-0.7%	-0.1	-0.05%	0	-1.6	-0.9%	-0.2	-0.09%	1
TDF	-9.6	-5.5%	0.0	-0.04%	-5.3	-3.1%	0.0	-0.03%	1	-3.7	-2.2%	-0.2	-0.15%	3	-0.6	-0.4%	-0.1	-0.04%	0
MS	-16.2	-8.1%	-0.1	-0.06%	-12.7	-6.4%	-0.1	-0.05%	5	-3.5	-1.9%	-0.2	-0.12%	8	0.0	0.0%	0.0	0.00%	2
CD	-305.5	-14.3%	-1.8	-0.10%	-207.9	-9.7%	-1.8	-0.08%	33	-75.0	-3.9%	-5.0	-0.26%	29	-22.5	-1.2%	-2.3	-0.12%	16
CDMG	-20.4	-9.3%	0.0	-0.07%	-16.5	-6.0%	0.0	-0.05%	7	-3.7	-3.2%	0.0	-0.21%	9	-0.1	-0.3%	0.0	-0.03%	0
IH	-22.7	-9.3%	-0.1	-0.07%	-14.7	-6.0%	-0.1	-0.05%	4	-7.3	-3.2%	-0.5	-0.21%	7	-0.7	-0.3%	-0.1	-0.03%	1
All	-4131.3	-15.4%	-26.8	-0.11%	-3105.6	-11.6%	-26.8	-0.10%	180	-514.1	-2.2%	-34.3	-0.14%	183	-511.5	-2.2%	-51.2	-0.22%	165

882 **APPENDIX**

883 **Appendix 1.** List of images used in the inventory. All Landsat images are natural look with geographic
884 reference. Landsat resolution 30 m; swath 185 km. Glacier extent in AD1870 was mapped from 16 Landsat 7
885 ETM+ SLC-on images from 2000-2001. Glacier extents in 1975 from Aniya (1988) map for the NPI (provided
886 as shapefiles by Masamu Aniya). Inventory in 1987 from 20 Landsat 4-5 images. Inventory in 2001 from 16
887 Landsat 7 ETM+ SLC-on images. Inventory in 2011 from Landsat 7 ETM+ SLC-OFF images.

Sensor	Image ID	Date	Path/Row
Landsat 7 ETM+ SLC-OFF	LE72320892011050EDC00	19/02/2011	232/89
Landsat 7 ETM+ SLC-OFF	LE72320902011050EDC00	19/02/2011	232/90
Landsat 7 ETM+ SLC-OFF	LE72320912011210COA00	29/07/2011	232/91
Landsat 7 ETM+ SLC-OFF	LE72320922011050EDC00	19/02/2011	232/92
Landsat 7 ETM+ SLC-OFF	LT52310932011299EDC01	26/10/2011	231/93
Landsat 7 ETM+ SLC-OFF	LE72320932011050EDC00	19/02/2011	232/93
Landsat 7 ETM+ SLC-OFF	LE72320942011050EDC00	19/02/2011	232/94
Landsat 7 ETM+ SLC-OFF	LE72310942011347EDC00	13/12/2011	231/94
Landsat 7 ETM+ SLC-OFF	LE72310952011299EDC00	26/10/2011	231/95
Landsat 7 ETM+ SLC-OFF	LE72310952011347COA00	13/12/2011	231/95
Landsat 7 ETM+ SLC-OFF	LE72320952011050EDC00	19/02/2011	231/95
Landsat 7 ETM+ SLC-OFF	LE72320952011274ASN00	01/10/2011	232/95
Landsat 7 ETM+ SLC-OFF	LE72310962010088EDC00	29/03/2010	231/96
Landsat 7 ETM+ SLC-OFF	LE72300972007249ASN00	06/09/2007	230/97
Landsat 7 ETM+ SLC-OFF	LE72290982010250EDC00	07/09/2010	229/98
Landsat 7 ETM+ SLC-OFF	LE72270982011095EDC00	05/04/2011	227/98
Landsat 7 ETM+ SLC-OFF	LE72270982010092EDC00	02/04/2010	227/98
Landsat 7 EMT+ SLC-on	p226r099_7f2001214_z19_ps742	14/12/2001	226/99
Landsat 7 EMT+ SLC-on	p227r0987f20020207_z19_pz742	07/02/2002	227/98
Landsat 7 EMT+ SLC-on	p228r098_7f20010331_z19_ps742	31/03/2001	228/98
Landsat 7 EMT+ SLC-on	p230r096_7f20010507_z18_ps742	07/05/2001	230/96
Landsat 7 EMT+ SLC-on	LE72300972001216EDC00	04/08/2001	230/97
Landsat 7 EMT+ SLC-on	p231r093_7f20010115_z18_ps742	15/01/2001	231/93
Landsat 7 EMT+ SLC-on	p231r094_7f20011027_z18_ps742	27/10/2001	231/94
Landsat 7 EMT+ SLC-on	p231r095_7f20011014_z18_ps742	14/10/2001	231/95
Landsat 7 EMT+ SLC-on	p232r089_7f20011208_z18_ps742	08/12/2001	232/89
Landsat 7 EMT+ SLC-on	p232r090_7f20011208_z18_ps742	08/12/2001	232/90
Landsat 7 EMT+ SLC-on	p232r091_7f20011208_z18_ps742	08/12/2001	232/91
Landsat 7 EMT+ SLC-on	p232r092_7f20010311_z18_ps742	03/11/2001	232/92
Landsat 7 EMT+ SLC-on	p232r093_7f20010311_z18_ps742	11/03/2001	232/93
Landsat 7 EMT+ SLC-on	p233r089_7f20011129_z18_ps742	29/11/2001	233/89
Landsat 7 EMT+ SLC-on	p233r090_7f20010403_z18_ps742	03/04/2001	233/90
Landsat 7 EMT+ SLC-on	P233r092_7f20000822_z18_ps74	22/08/2000	233/92
Landsat 4-5 TM	LT52320891986053AAA03	22/02/1989	232/89
Landsat 4-5 TM	LT52320901986229AAA08	17/08/1986	232/90
Landsat 4-5 TM	LT52320911986229AAA08	17/08/1986	232/91
Landsat 4-5 TM	LT52310911986270AAA04	27/09/1986	231/91
Landsat 4-5 TM	LT52310911986270AAA04	27/09/1986	231/91
Landsat 4-5 TM	LT52320911986117XXX02	27/14/1986	232/91
Landsat 4-5 TM	LT52320921987040XXX02	15/09/1987	232/92
Landsat 4-5 TM	LT52310931986270AAA03	27/09/1986	231/93
Landsat 4-5 TM	LT523209311987040XXX02	09/02/1987	232/93
Landsat 4-5 TM	LT52310941986270AAA11	27/09/1986	231/94
Landsat 4-5 TM	LT52320941986277XXX02	04/10/1986	232/94
Landsat 4-5 TM	LT52310951985027AAA03	27/01/1985	231/95

Landsat 4-5 TM	LT52310951986270AAA02	27/09/1986	231/95
Landsat 4-5 TM	LT52310961986014XXX04	14/01/1986	231/96
Landsat 4-5 TM	LT52310961986014XXX04	14/01/1986	231/96
Landsat 4-5 TM	LT52300971986279XXX03	06/10/1986	230/97
Landsat 4-5 TM	LT52280981986057XXX02	26/02/1986	228/98
Landsat 4-5 TM	LT52270981986258XXX03	15/06/1986	227/98
Landsat 4-5 TM	LT52270981985143AAA02	23/05/1985	227/98
Landsat 4-5 TM	LT52280981986057XXX02	26/02/1986	228/98

888

889 **Appendix 2**. List of NASA SRTM DEM V4.1 tiles downloaded for this study from http://srtm.csi.cgiar.org.
890 These images have a swath of 225 km and a resolution of 90 m. All images date from February 2000.

Path/Row
srtm_21-22
srtm_21_23
srtm_22_21
srtm_22_22
srtm_22_23
srtm_22_24
srtm_23_21
srtm_23_22
srtm_23_23
srtm_23_24
srtm_24_23

891

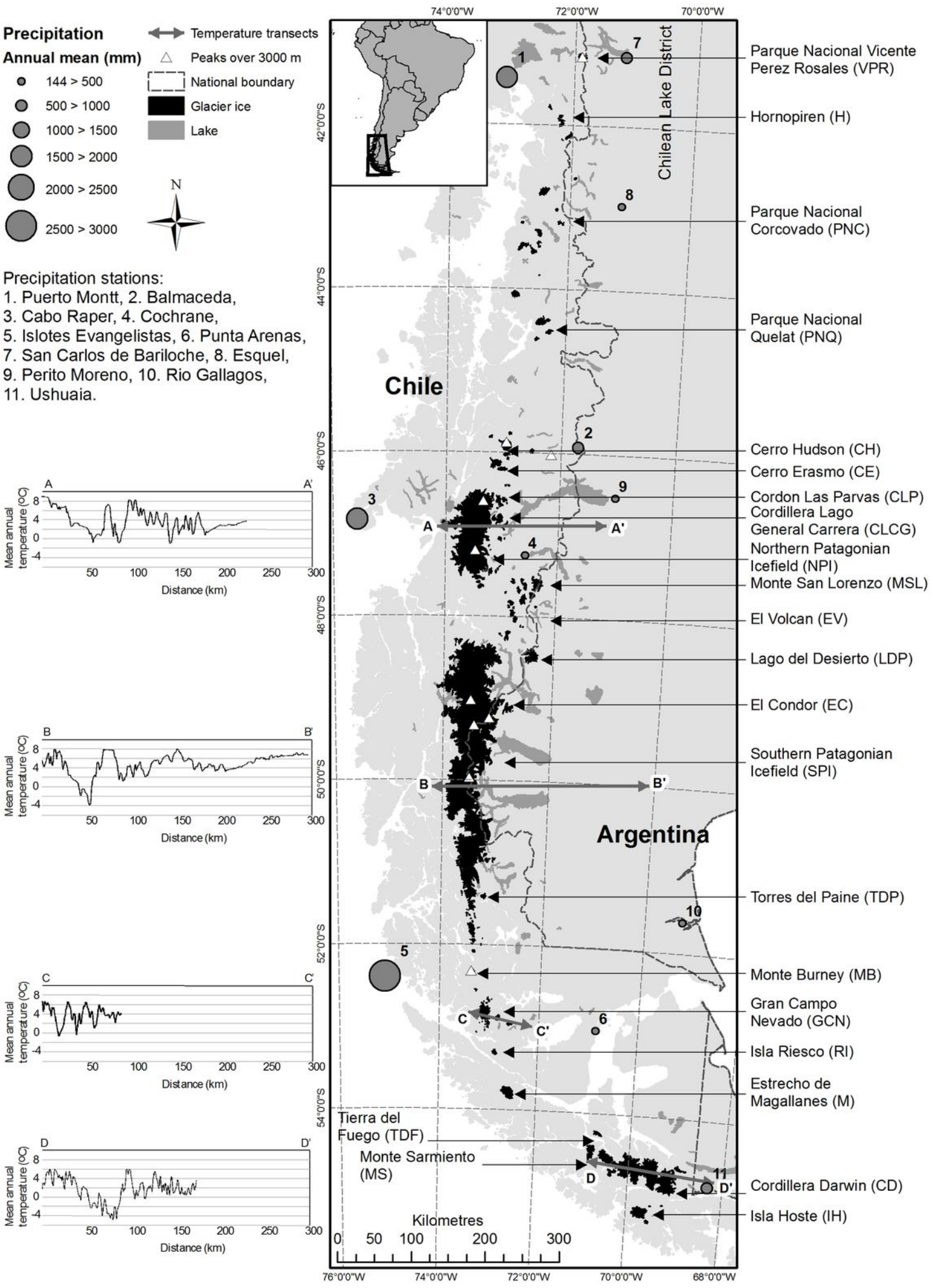
Precipitation
Annual mean (mm)
144 > 500
500 > 1000
1000 > 1500
1500 > 2000
2000 > 2500
2500 > 3000
Temperature transects
Peaks over 3000 m
National boundary
Glacier ice
Lake
N
Precipitation stations:
1. Puerto Montt, 2. Balmaceda,
3. Cabo Raper, 4. Cochrane,
5. Islotes Evangelistas, 6. Punta Arenas,
7. San Carlos de Bariloche, 8. Esquel,
9. Perito Moreno, 10. Rio Gallagos,
11. Ushuaia.
Mean annual temperature (ºC)
Distance (km)
Chilean Lake District
Chile
Argentina
Parque Nacional Vicente Perez Rosales (VPR)
Hornopiren (H)
Parque Nacional Corcovado (PNC)
Parque Nacional Quelat (PNQ)
Cerro Hudson (CH)
Cerro Erasmo (CE)
Cordon Las Parvas (CLP)
Cordillera Lago General Carrera (CLCG)
Northern Patagonian Icefield (NPI)
Monte San Lorenzo (MSL)
El Volcan (EV)
Lago del Desierto (LDP)
El Condor (EC)
Southern Patagonian Icefield (SPI)
Torres del Paine (TDP)
Monte Burney (MB)
Gran Campo Nevado (GCN)
Isla Riesco (RI)
Estrecho de Magallanes (M)
Tierra del Fuego (TDF)
Monte Sarmiento (MS)
Cordillera Darwin (CD)
Isla Hoste (IH)
Kilometres
74°0'0"W
72°0'0"W
70°0'0"W
76°0'0"W
68°0'0"W
42°0'0"S
44°0'0"S
46°0'0"S
48°0'0"S
50°0'0"S
52°0'0"S
54°0'0"S

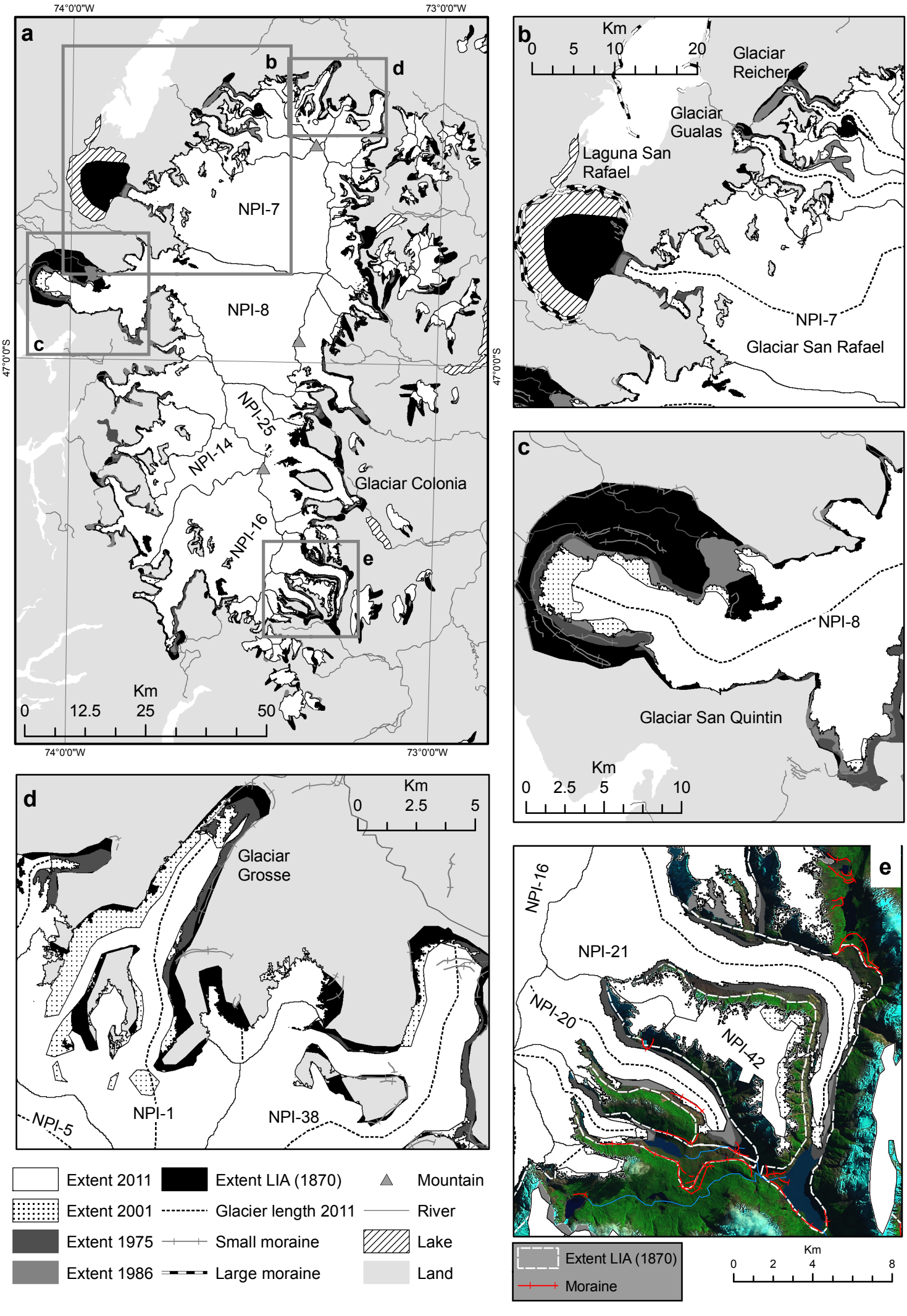
a
b
c
d
e
74°0'0"W
73°0'0"W
47°0'0"S
NPI-7
NPI-8
NPI-25
NPI-14
NPI-16
Glaciar Colonia
Km
0 12.5 25 50
Km
0 5 10 20
Glaciar Reicher
Glaciar Gualas
Laguna San Rafael
NPI-7
Glaciar San Rafael
Glaciar San Quintin
NPI-8
Km
0 2.5 5 10
Glaciar Grosse
NPI-1
NPI-38
NPI-5
Km
0 2.5 5
NPI-16
NPI-21
NPI-20
NPI-42
Extent 2011
Extent 2001
Extent 1975
Extent 1986
Extent LIA (1870)
Glacier length 2011
Small moraine
Large moraine
Mountain
River
Lake
Land
Extent LIA (1870)
Moraine
Km
0 2 4 8

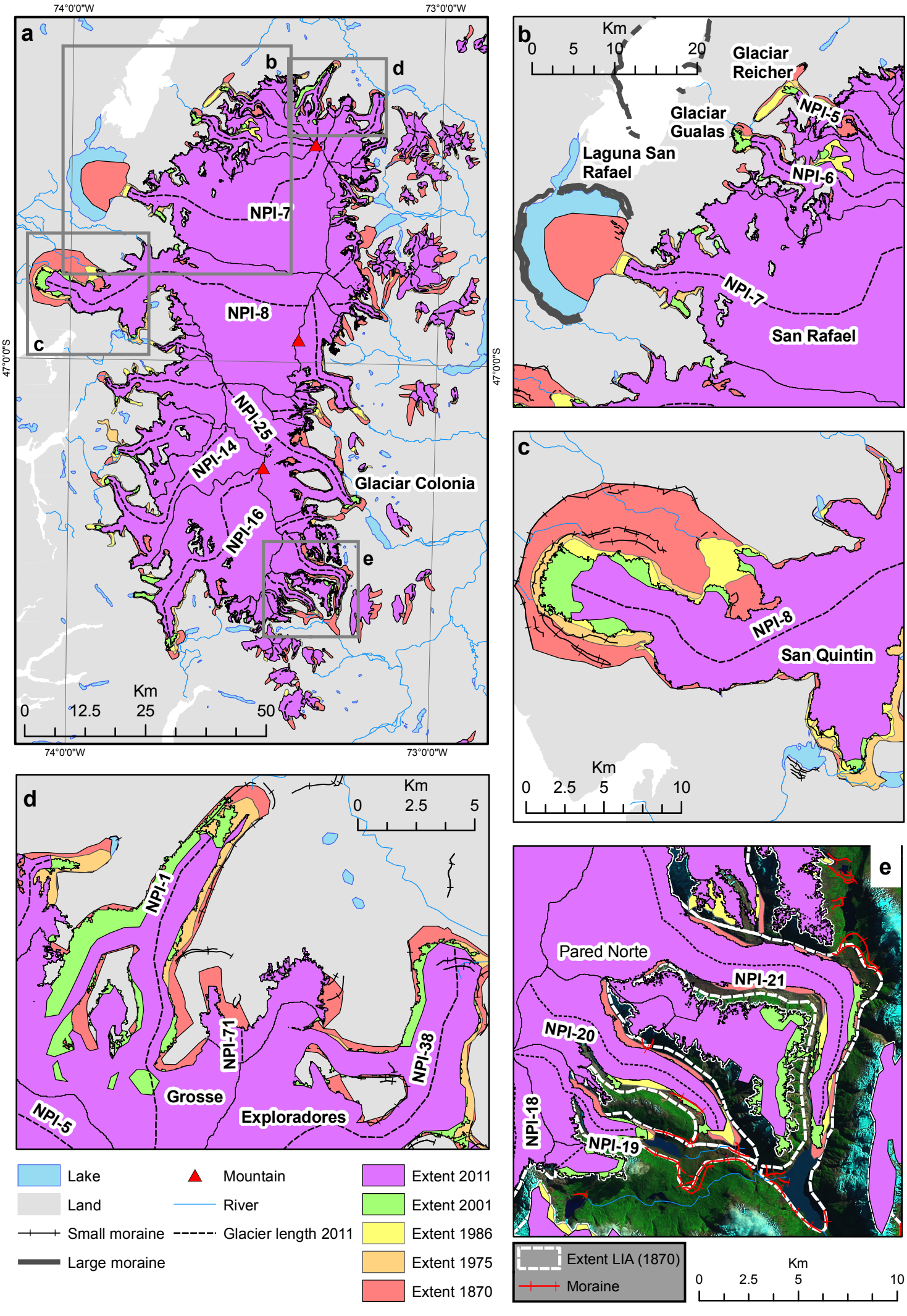
a
b
c
d
e
74°0'0"W
73°0'0"W
47°0'0"S
NPI-7
NPI-8
NPI-25
NPI-14
NPI-16
Glaciar Colonia
Km
0 12.5 25 50
Glaciar Reicher
Glaciar Gualas
Laguna San Rafael
NPI-5
NPI-6
San Rafael
San Quintin
NPI-1
NPI-71
NPI-38
Grosse
Exploradores
Pared Norte
NPI-21
NPI-20
NPI-18
NPI-19
Lake
Land
Small moraine
Large moraine
Mountain
River
Glacier length 2011
Extent 2011
Extent 2001
Extent 1986
Extent 1975
Extent 1870
Extent LIA (1870)
Moraine

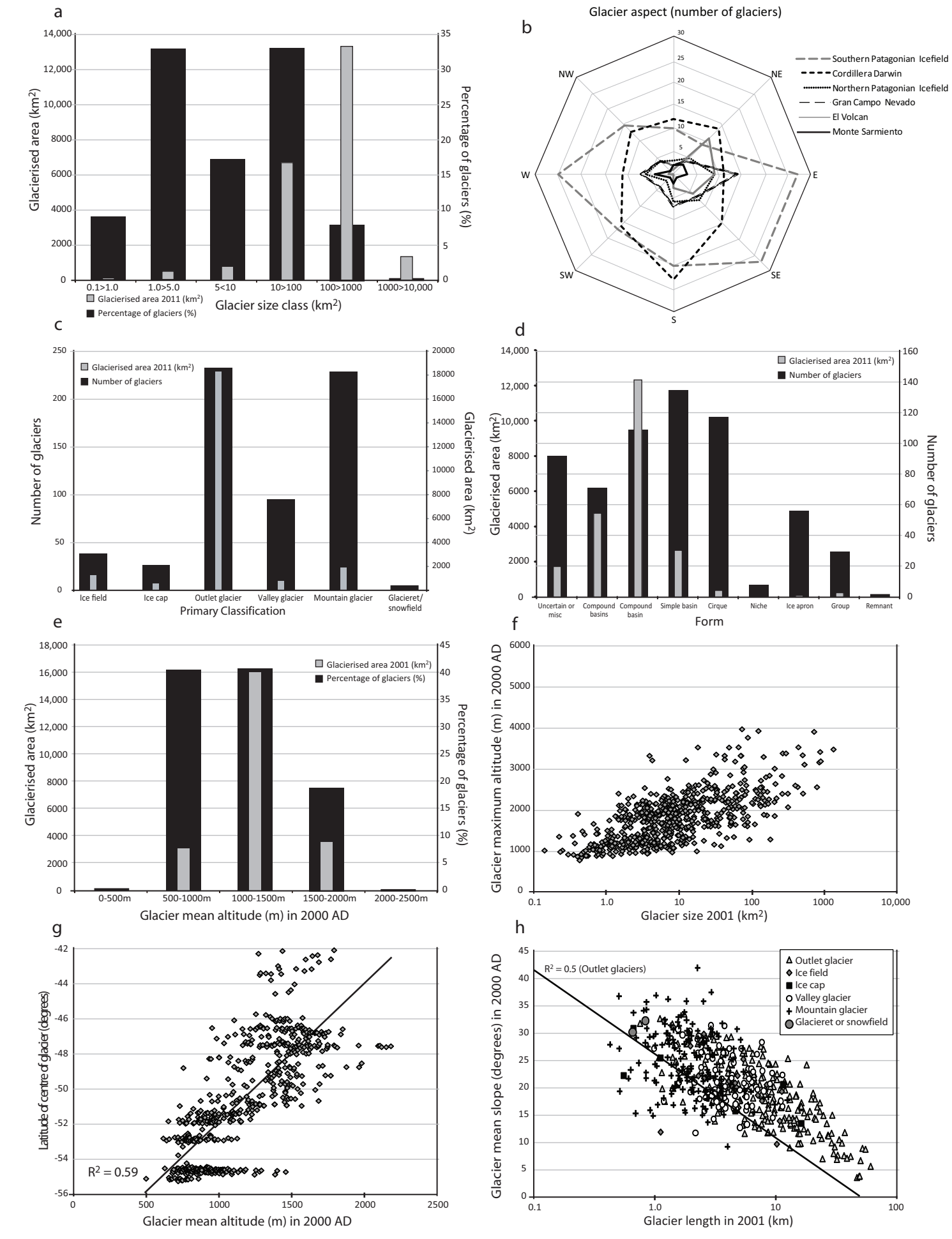
a
Glacierised area (km²)
Percentage of glaciers (%)
0.1>1.0
1.0>5.0
5<10
10>100
100>1000
1000>10,000
Glacierised area 2011 (km²)
Percentage of glaciers (%)
Glacier size class (km²)
b
Glacier aspect (number of glaciers)
NW
NE
W
E
SW
SE
S
Southern Patagonian Icefield
Cordillera Darwin
Northern Patagonian Icefield
Gran Campo Nevado
El Volcan
Monte Sarmiento
c
Glacierised area 2011 (km²)
Number of glaciers
Number of glaciers
Glacierised area (km²)
Ice field
Ice cap
Outlet glacier
Valley glacier
Mountain glacier
Glacieret/ snowfield
Primary Classification
d
Glacierised area 2011 (km²)
Number of glaciers
Glacierised area (km²)
Number of glaciers
Uncertain or misc
Compound basins
Compound basin
Simple basin
Cirque
Niche
Ice apron
Group
Remnant
Form
e
Glacierised area 2001 (km²)
Percentage of glaciers (%)
Glacierised area (km²)
Percentage of glaciers (%)
0-500m
500-1000m
1000-1500m
1500-2000m
2000-2500m
Glacier mean altitude (m) in 2000 AD
f
Glacier maximum altitude (m) in 2000 AD
Glacier size 2001 (km²)
g
Latitude of centre of glacier (degrees)
R² = 0.59
Glacier mean altitude (m) in 2000 AD
h
R² = 0.5 (Outlet glaciers)
Outlet glacier
Ice field
Ice cap
Valley glacier
Mountain glacier
Glacieret or snowfield
Glacier mean slope (degrees) in 2000 AD
Glacier length in 2001 (km)

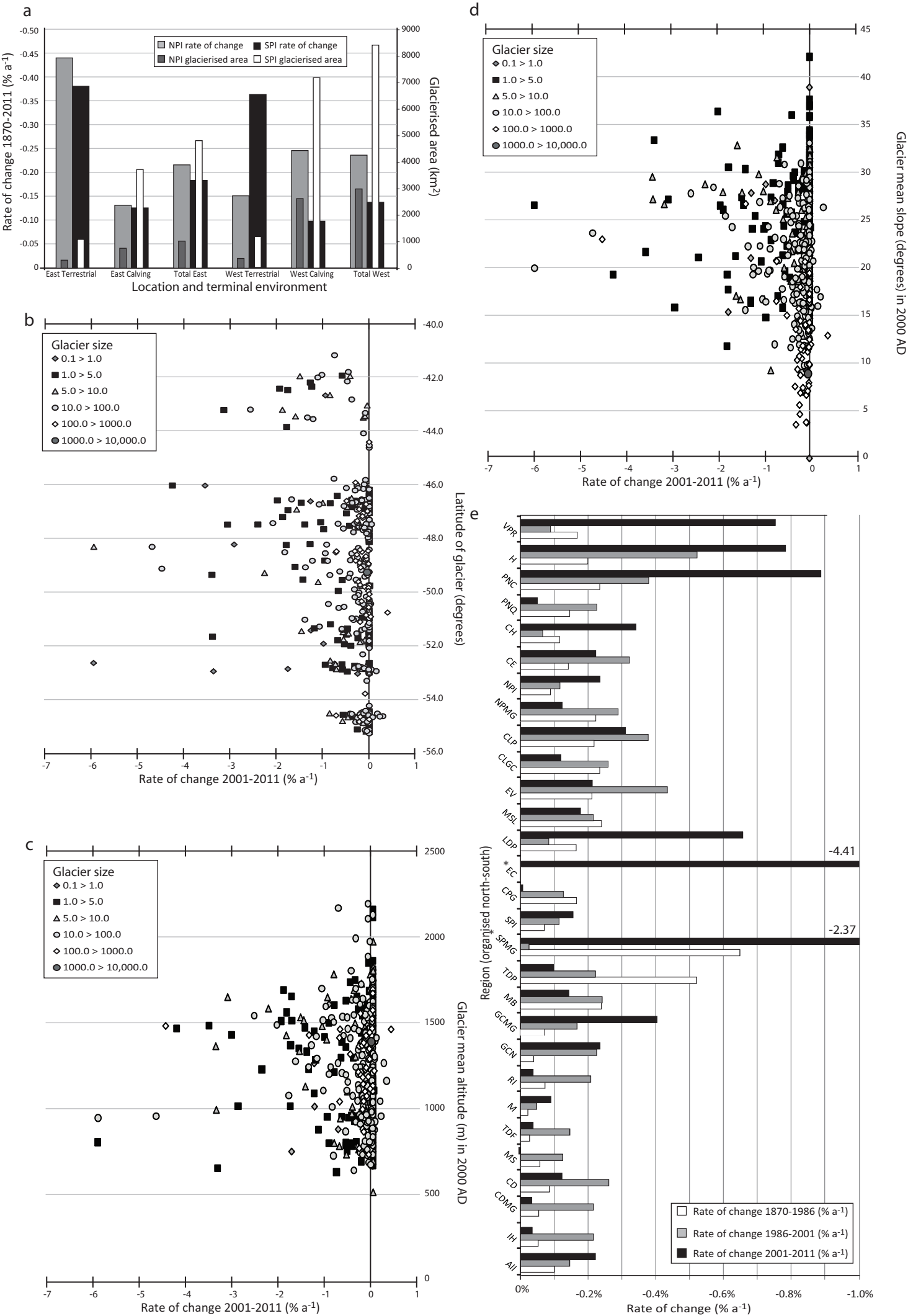
a
NPI rate of change
SPI rate of change
NPI glacierised area
SPI glacierised area
Rate of change 1870-2011 (% a-1)
Glacierised area (km2)
East Terrestrial
East Calving
Total East
West Terrestrial
West Calving
Total West
Location and terminal environment
b
Glacier size
0.1 > 1.0
1.0 > 5.0
5.0 > 10.0
10.0 > 100.0
100.0 > 1000.0
1000.0 > 10,000.0
Latitude of glacier (degrees)
Rate of change 2001-2011 (% a-1)
c
Glacier mean altitude (m) in 2000 AD
d
Glacier mean slope (degrees) in 2000 AD
e
Region (organised north-south)
VPR
H
PNC
PNQ
CH
CE
NPI
NPMG
CLP
CLGC
EV
MSL
LDP
EC
CPG
SPI
SPMG
TDP
MB
GCMG
GCN
RI
M
TDF
MS
CD
CDMG
IH
All
-4.41
-2.37
Rate of change 1870-1986 (% a-1)
Rate of change 1986-2001 (% a-1)
Rate of change 2001-2011 (% a-1)
Rate of change (% a-1)

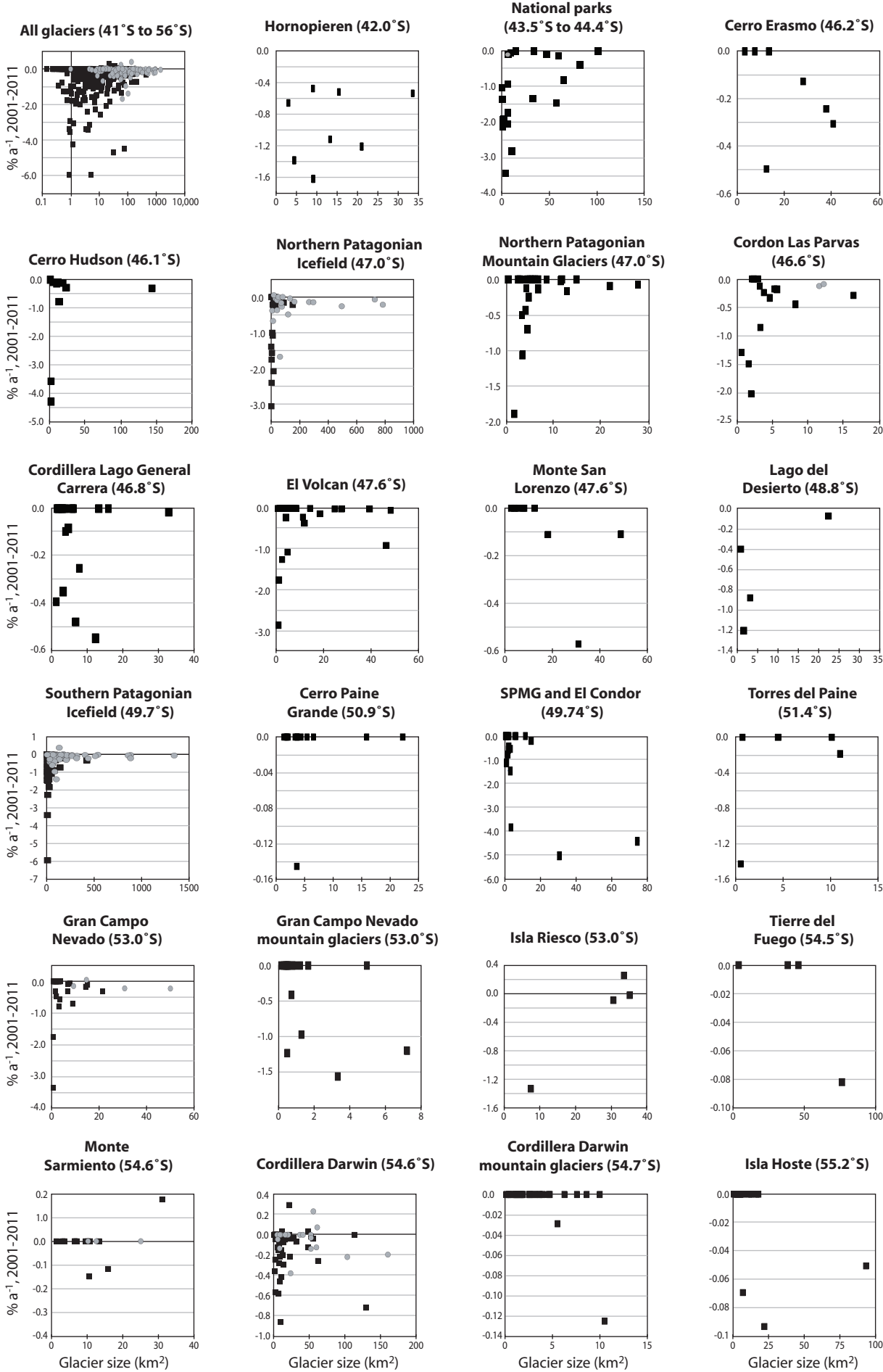
All glaciers (41˚S to 56˚S)
Hornopieren (42.0˚S)
National parks (43.5˚S to 44.4˚S)
Cerro Erasmo (46.2˚S)
Cerro Hudson (46.1˚S)
Northern Patagonian Icefield (47.0˚S)
Northern Patagonian Mountain Glaciers (47.0˚S)
Cordon Las Parvas (46.6˚S)
Cordillera Lago General Carrera (46.8˚S)
El Volcan (47.6˚S)
Monte San Lorenzo (47.6˚S)
Lago del Desierto (48.8˚S)
Southern Patagonian Icefield (49.7˚S)
Cerro Paine Grande (50.9˚S)
SPMG and El Condor (49.74˚S)
Torres del Paine (51.4˚S)
Gran Campo Nevado (53.0˚S)
Gran Campo Nevado mountain glaciers (53.0˚S)
Isla Riesco (53.0˚S)
Tierre del Fuego (54.5˚S)
Monte Sarmiento (54.6˚S)
Cordillera Darwin (54.6˚S)
Cordillera Darwin mountain glaciers (54.7˚S)
Isla Hoste (55.2˚S)
% a-1, 2001-2011
Glacier size (km2)

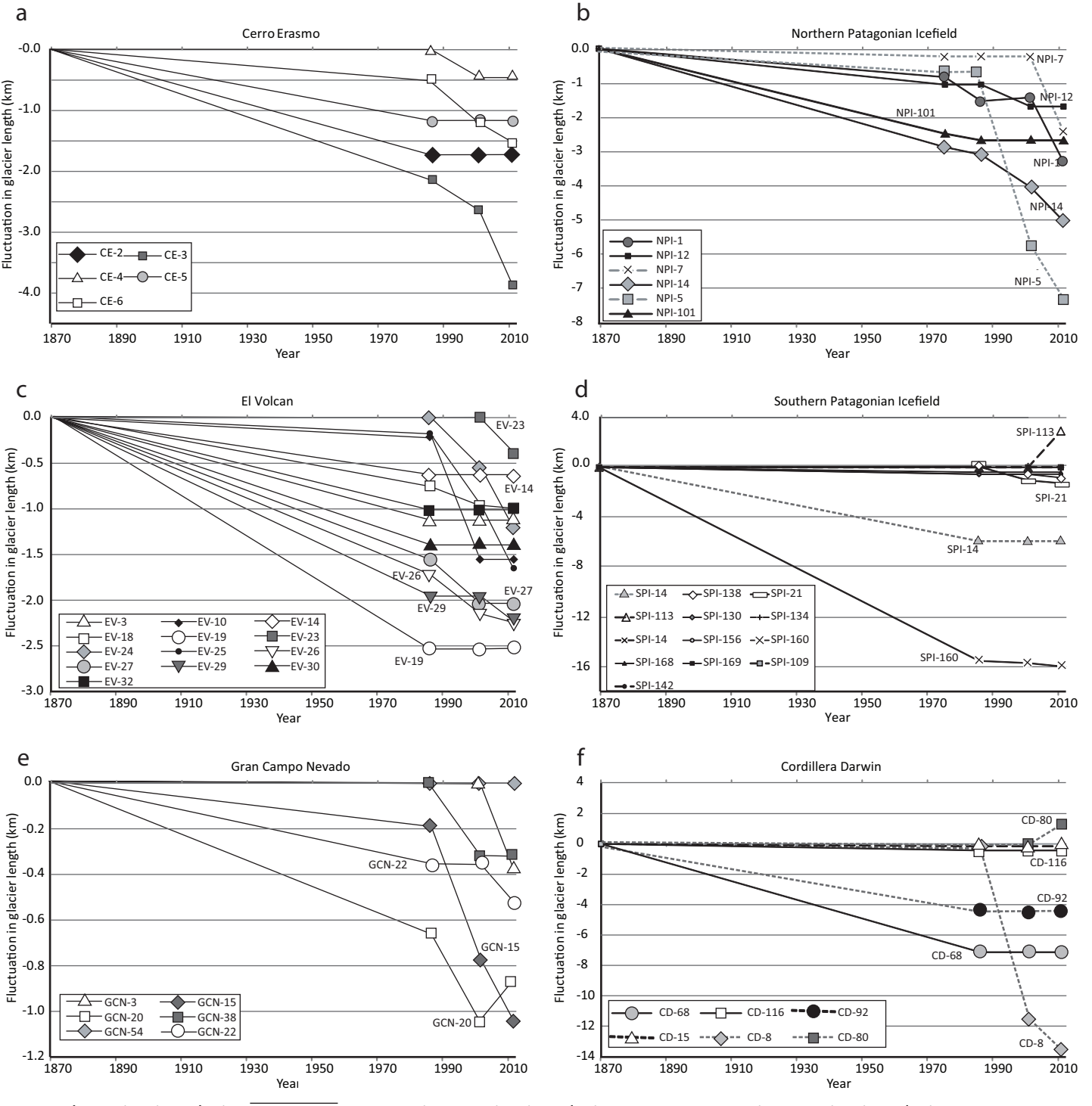
a
Cerro Erasmo
Fluctuation in glacier length (km)
Year
CE-2
CE-3
CE-4
CE-5
CE-6
b
Northern Patagonian Icefield
NPI-7
NPI-12
NPI-101
NPI-14
NPI-5
NPI-1
NPI-12
NPI-7
NPI-14
NPI-5
NPI-101
c
El Volcan
EV-23
EV-14
EV-26
EV-27
EV-29
EV-19
EV-3
EV-10
EV-14
EV-18
EV-19
EV-23
EV-24
EV-25
EV-26
EV-27
EV-29
EV-30
EV-32
d
Southern Patagonian Icefield
SPI-113
SPI-21
SPI-14
SPI-160
SPI-14
SPI-138
SPI-21
SPI-113
SPI-130
SPI-134
SPI-14
SPI-156
SPI-160
SPI-168
SPI-169
SPI-109
SPI-142
e
Gran Campo Nevado
GCN-22
GCN-15
GCN-20
GCN-3
GCN-15
GCN-20
GCN-38
GCN-54
GCN-22
f
Cordillera Darwin
CD-80
CD-116
CD-92
CD-68
CD-8
CD-68
CD-116
CD-92
CD-15
CD-8
CD-80
Land-terminating glacier
Lacustrine-terminating glacier
Marine-terminating glacier

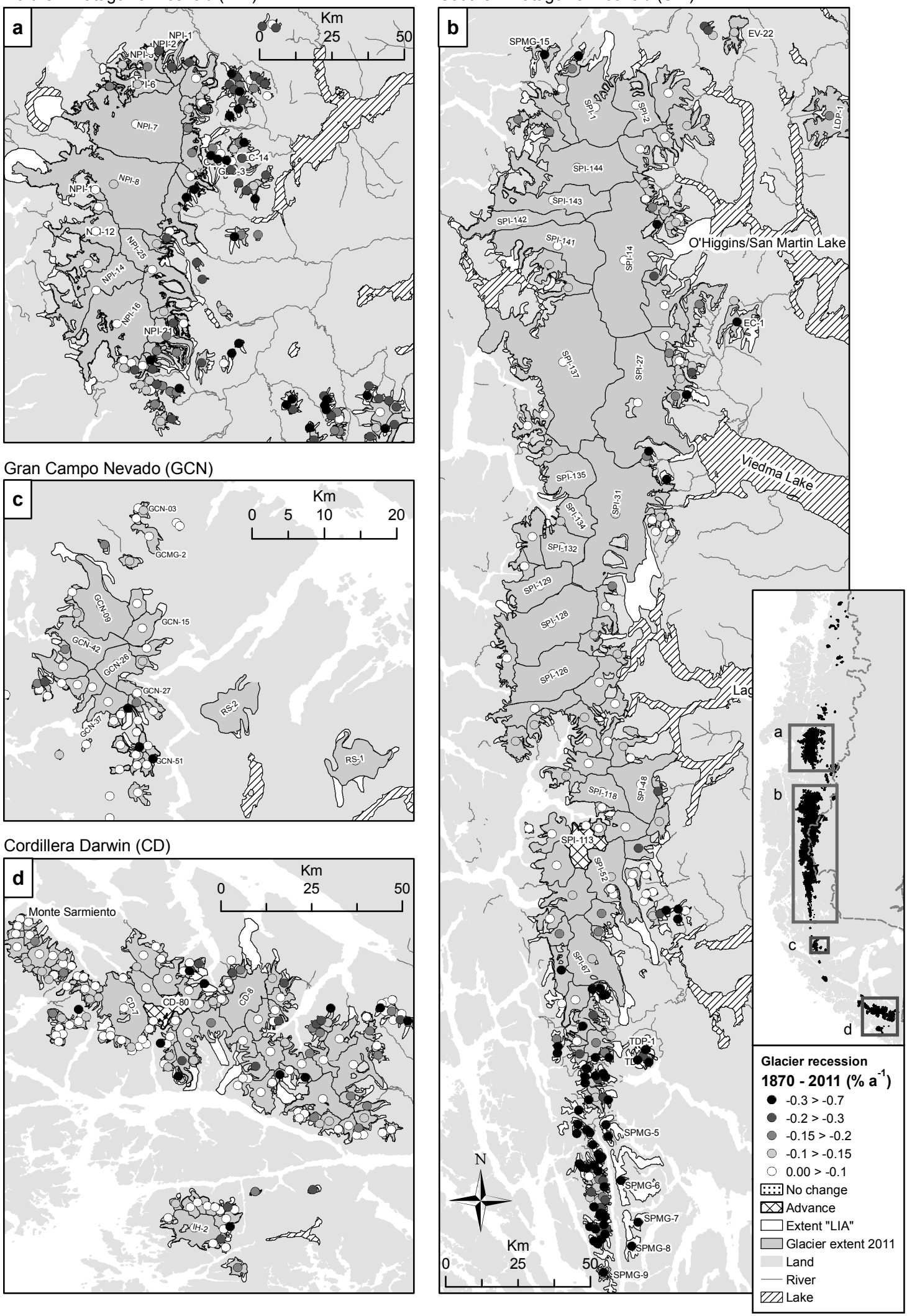
Northern Patagonian Icefield (NPI)
a
Km
0
25
50
NPI-1
NPI-2
NPI-3
NPI-6
NPI-7
NPI-8
NPI-12
NPI-25
NPI-14
NPI-16
NPI-21
Gran Campo Nevado (GCN)
c
Km
0
5
10
20
GCN-03
GCMG-2
GCN-09
GCN-15
GCN-42
GCN-26
GCN-27
GCN-37
GCN-51
RS-2
RS-1
Cordillera Darwin (CD)
d
Km
0
25
50
Monte Sarmiento
CD-7
CD-80
CD-8
IH-2
Southern Patagonian Icefield (SPI)
b
SPMG-15
EV-22
SPI-1
SPI-2
LDP-1
SPI-144
SPI-143
SPI-142
SPI-141
SPI-14
O'Higgins/San Martin Lake
EC-1
SPI-137
SPI-27
Viedma Lake
SPI-135
SPI-31
SPI-134
SPI-132
SPI-129
SPI-128
SPI-126
SPI-118
SPI-48
SPI-113
SPI-52
SPI-67
TDP-1
SPMG-5
SPMG-6
SPMG-7
SPMG-8
SPMG-9
N
Km
0
25
50
a
b
c
d
Glacier recession
1870 - 2011 (% a-1)
-0.3 > -0.7
-0.2 > -0.3
-0.15 > -0.2
-0.1 > -0.15
0.00 > -0.1
No change
Advance
Extent "LIA"
Glacier extent 2011
Land
River
Lake

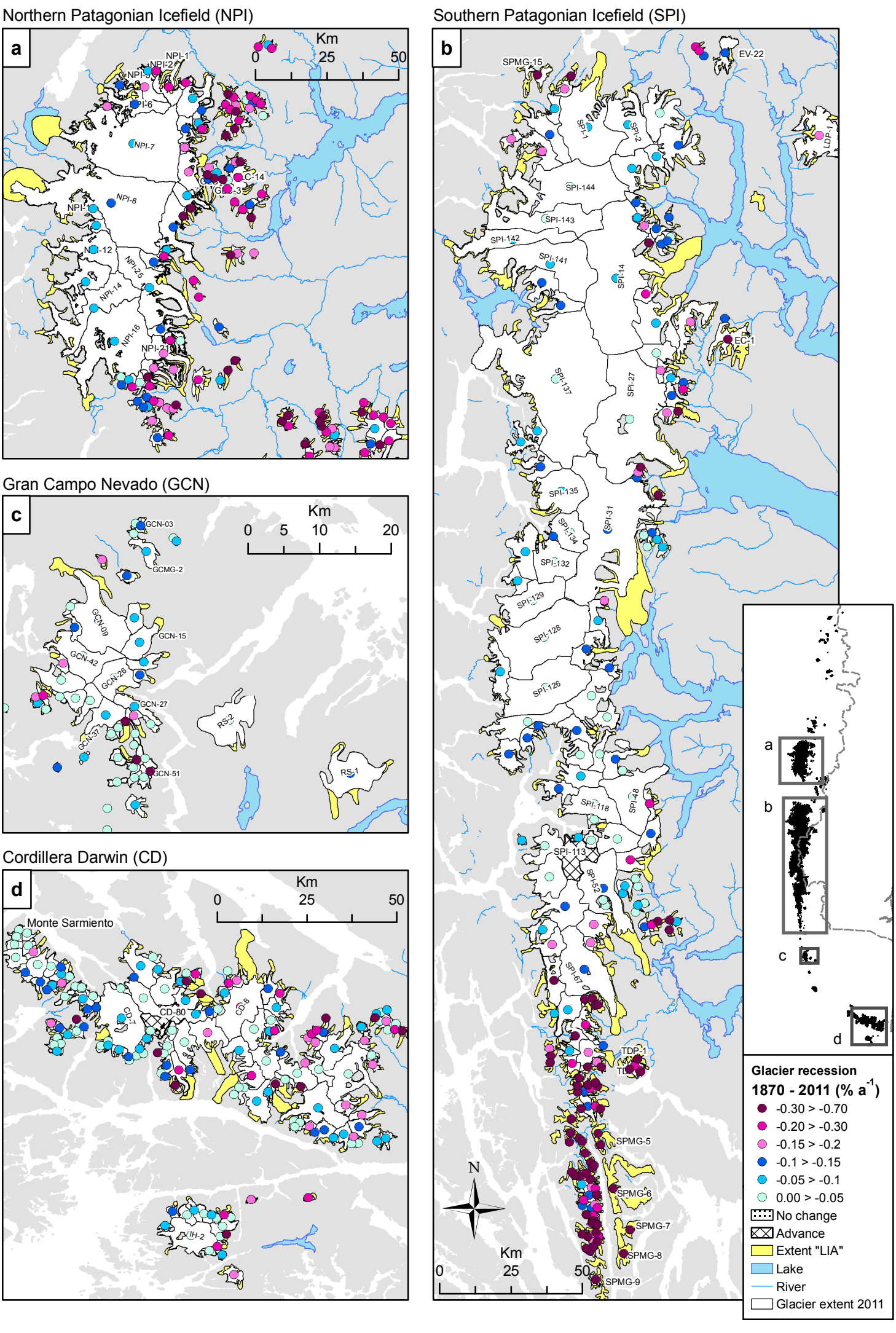
Northern Patagonian Icefield (NPI)
a
Km
0
25
50
NPI-1
NPI-2
NPI-6
NPI-7
NPI-8
NPI-12
NPI-25
NPI-14
NPI-16
NPI-21
C-14
Gran Campo Nevado (GCN)
c
Km
0
5
10
20
GCN-03
GCMG-2
GCN-09
GCN-15
GCN-42
GCN-26
GCN-27
GCN-37
GCN-51
RS-2
RS-1
Cordillera Darwin (CD)
d
Km
0
25
50
Monte Sarmiento
CD-7
CD-80
CD-8
CH-2
Southern Patagonian Icefield (SPI)
b
SPMG-15
EV-22
SPI-1
SPI-2
LDP-1
SPI-144
SPI-143
SPI-142
SPI-141
SPI-14
EC-1
SPI-137
SPI-27
SPI-135
SPI-31
SPI-134
SPI-132
SPI-129
SPI-128
SPI-126
SPI-118
SPI-48
SPI-113
SPI-52
SPI-67
TDP-1
TDP-2
SPMG-5
SPMG-6
SPMG-7
SPMG-8
SPMG-9
N
Km
0
25
50
a
b
c
d
Glacier recession
1870 - 2011 (% a-1)
-0.30 > -0.70
-0.20 > -0.30
-0.15 > -0.2
-0.1 > -0.15
-0.05 > -0.1
0.00 > -0.05
No change
Advance
Extent "LIA"
Lake
River
Glacier extent 2011

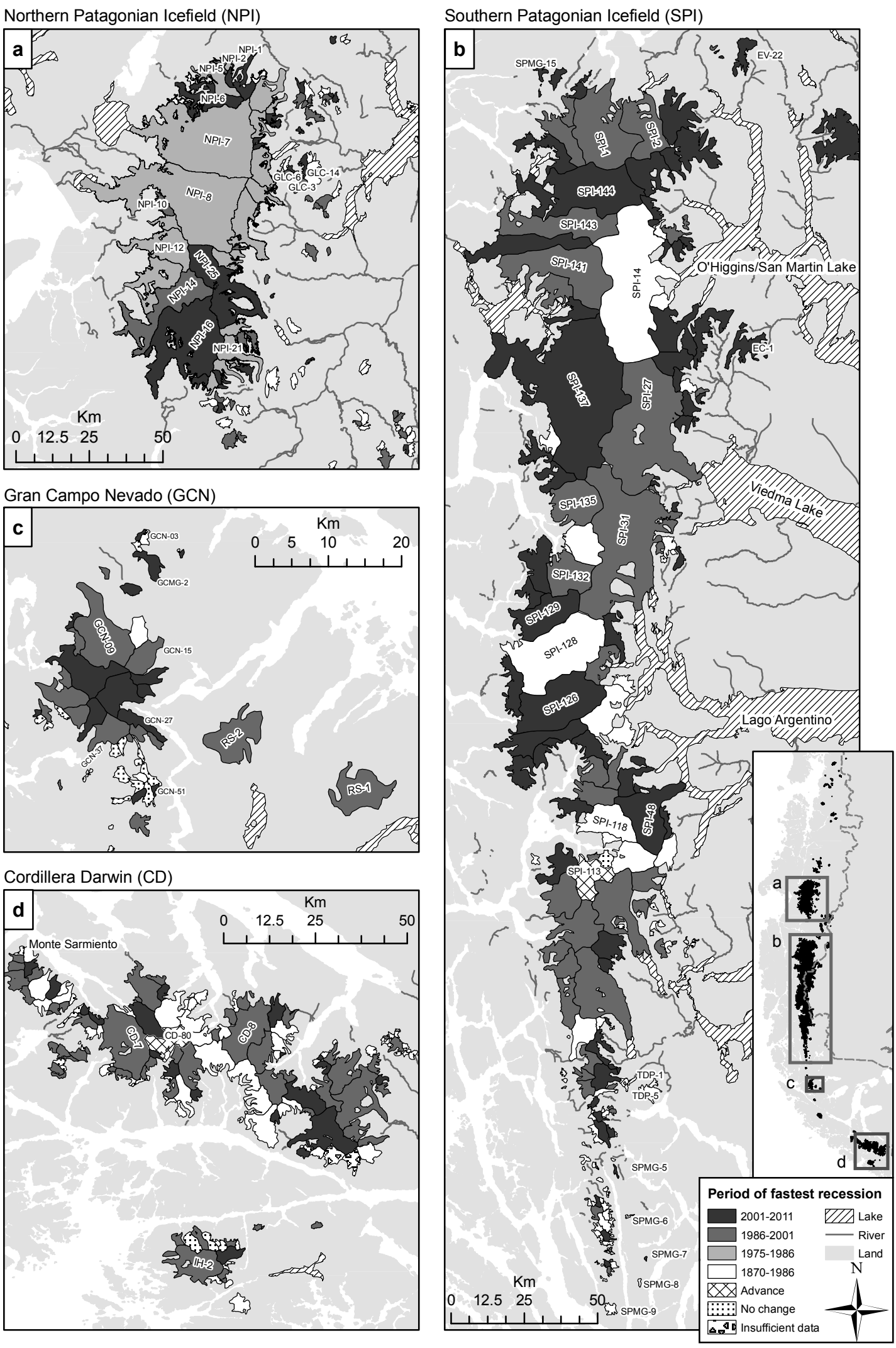
Northern Patagonian Icefield (NPI)
a
NPI-1
NPI-2
NPI-5
NPI-6
NPI-7
NPI-8
NPI-10
NPI-12
NPI-25
NPI-14
NPI-16
NPI-21
GLC-6
GLC-14
GLC-3
Km
0 12.5 25 50
Gran Campo Nevado (GCN)
c
Km
0 5 10 20
GCN-03
GCMG-2
GCN-09
GCN-15
GCN-27
GCN-37
GCN-51
RS-2
RS-1
Cordillera Darwin (CD)
d
Km
0 12.5 25 50
Monte Sarmiento
CD-7
CD-80
CD-8
IH-2
Southern Patagonian Icefield (SPI)
b
SPMG-15
EV-22
SPI-1
SPI-2
SPI-144
SPI-143
SPI-141
SPI-14
O'Higgins/San Martin Lake
EC-1
SPI-137
SPI-27
Viedma Lake
SPI-135
SPI-31
SPI-132
SPI-129
SPI-128
SPI-126
Lago Argentino
SPI-48
SPI-118
SPI-113
TDP-1
TDP-5
SPMG-5
SPMG-6
SPMG-7
SPMG-8
SPMG-9
Km
0 12.5 25 50
a
b
c
d
Period of fastest recession
2001-2011
1986-2001
1975-1986
1870-1986
Advance
No change
Insufficient data
Lake
River
Land
N

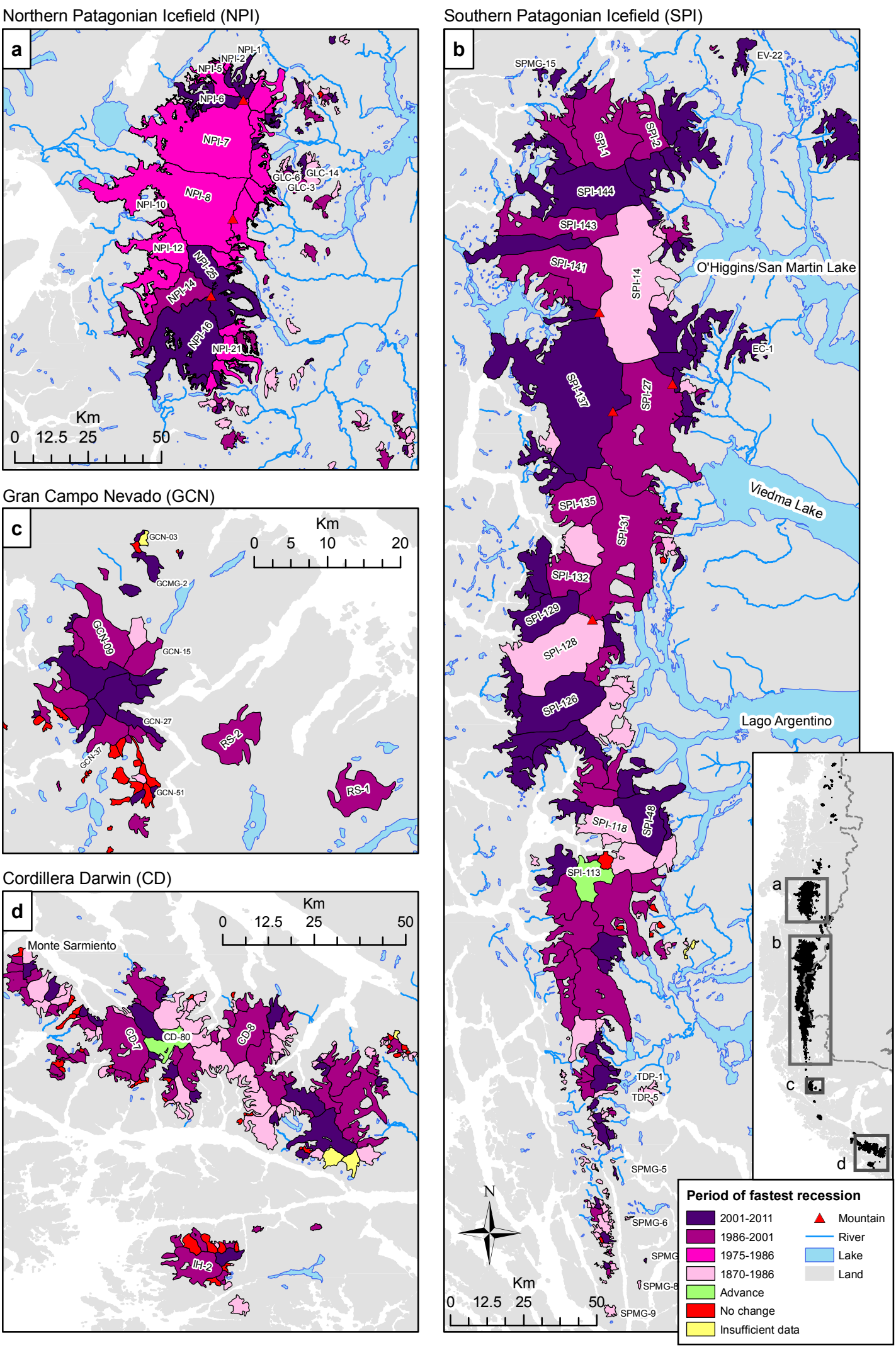
Northern Patagonian Icefield (NPI)
a
NPI-1
NPI-2
NPI-5
NPI-6
NPI-7
NPI-8
NPI-10
NPI-12
NPI-25
NPI-14
NPI-16
NPI-21
GLC-6
GLC-14
GLC-3
Km
0 12.5 25 50
Gran Campo Nevado (GCN)
c
Km
0 5 10 20
GCN-03
GCMG-2
GCN-09
GCN-15
GCN-27
GCN-37
GCN-51
RS-2
RS-1
Cordillera Darwin (CD)
d
Km
0 12.5 25 50
Monte Sarmiento
CD-7
CD-80
CD-8
IH-2
Southern Patagonian Icefield (SPI)
b
SPMG-15
EV-22
SPI-1
SPI-2
SPI-144
SPI-143
SPI-141
SPI-14
O'Higgins/San Martin Lake
EC-1
SPI-137
SPI-27
Viedma Lake
SPI-135
SPI-31
SPI-132
SPI-129
SPI-128
SPI-126
Lago Argentino
SPI-118
SPI-48
SPI-113
TDP-1
TDP-5
SPMG-5
SPMG-6
SPMG-8
SPMG-9
N
Km
0 12.5 25 50
a
b
c
d
Period of fastest recession
2001-2011
1986-2001
1975-1986
1870-1986
Advance
No change
Insufficient data
Mountain
River
Lake
Land